The Plant Cell, Vol. 30: 2057–2081, September 2018, www.plantcell.org © 2018 ASPB.



# Glucose Uptake via STP Transporters Inhibits in Vitro Pollen Tube Growth in a HEXOKINASE1-Dependent Manner in *Arabidopsis thaliana*

**Theresa Rottmann, Carolin Fritz,[1] Norbert Sauer, and Ruth Stadler[2]**

Molecular Plant Physiology, Department of Biology, Friedrich-Alexander University Erlangen-Nuremberg, 91054 Erlangen, Germany

ORCID IDs: 0000-0003-3242-6674 (T.R.); 0000-0001-7514-5747 (C.F.); 0000-0003-4357-2079 (N.S.); 0000-0002-3103-6343 (R.S.)

**Pollen tube growth requires a high amount of metabolic energy and precise targeting toward the ovules. Sugars, especially glucose, can serve as nutrients and as signaling molecules. Unexpectedly, in vitro assays revealed an inhibitory effect of glucose on pollen tube elongation, contradicting the hypothesis that monosaccharide uptake is a source of nutrition for growing pollen tubes. Measurements with Förster resonance energy transfer-based nanosensors revealed that glucose is taken up into pollen tubes and that the intracellular concentration is in the low micromolar range. Pollen tubes of *stp4-6-8-9-10-11* sextuple knockout plants generated by crossings and CRISPR/Cas9 showed only a weak response to glucose, indicating that glucose uptake into pollen tubes is mediated mainly by these six monosaccharide transporters of the SUGAR TRANSPORT PROTEIN (STP) family. Analyses of *HEXOKINASE1* (*HXK1*) showed a strong expression of this gene in pollen. Together with the glucose insensitivity and altered semi-in vivo growth rate of pollen tubes from *hxk1* knockout lines, this strongly suggests that glucose is an important signaling molecule for pollen tubes, is taken up by STPs, and detected by HXK1. Equimolar amounts of fructose abolish the inhibitory effect of glucose indicating that only an excess of glucose is interpreted as a signal. This provides a possible model for the discrimination of signaling and nutritional sugars.**

## INTRODUCTION

Successful reproduction in angiosperms not only requires the deposition of pollen on a compatible stigma but also the transport of the immotile sperm cells to the egg cells that are localized inside the ovary. Depending on the morphology of the pistil the distance between the pollen grain on the stigma and the egg cell can be as far as 30 cm (Bedinger, 1992). To cover this distance, the pollen grain germinates and forms a pollen tube by elongation and tip growth of the vegetative cell. The extending pollen tube penetrates the stigma, grows through the transmitting tract, and finally enters the ovule through the micropyle and thus delivers the two sperm cells to their place of destination. Eventually, rupture of the pollen tube releases both sperm cells; one fuses with the egg cell and one with the central cell giving rise to the embryo and the endosperm, respectively. Elongating by tip growth, pollen tubes can reach growth rates up to 1 cm/h (Bedinger, 1992). This rapid growth process consumes a high amount of metabolic energy. Besides respiration the synthesis of cell wall material from UDP-glucose and its transport to the pollen tube tip are the major energy- and carbohydrate-consuming processes during pollen tube growth (Schlüpmann et al., 1994; Derksen et al., 1995). As pollen are photosynthetically inactive, they are preloaded with storage compounds during microgametogenesis. In *Arabidopsis thaliana*, SWEET8/RUPTURED POLLEN GRAIN1 probably releases glucose from the tapetum cells that surround the developing pollen grains in the anthers (Guan et al., 2008). Subsequent sugar uptake into pollen grains might be mediated by SUGAR TRANSPORT PROTEIN2 (STP2) as the expression of the respective gene is highly induced in developing pollen grains (Truernit et al., 1999). Mature pollen grains contain lipid bodies (Regan and Moffatt, 1990) and carbohydrates, especially starch within amyloplasts but also sucrose, glucose, or fructose in varying concentrations (Speranza et al., 1997). It has been proposed that these internal reserves are sufficient to sustain pollen germination and initial tube growth (Read et al., 1993), but several lines of evidence indicate that pollen tubes take up additional carbohydrates from the apoplast of the transmitting tract during growth. The glandular tissue lining the stigma surface and stylar canal of lily pistils secretes an exudate containing ~90 to 95% carbohydrates (Loewus and Labarca, 1973) and in the stylar fluids of petunia (*Petunia hybrida*) pistils sucrose, glucose, and fructose are available to the pollen tube (Konar and Linskens, 1966), indicating that the maternal sporophytic tissue not only provides directional cues but also nutrients for the growing pollen tubes. This is further underlined by the requirement of high sugar concentrations in the medium for successful germination and tube growth of pollen of different species in vitro (Kost et al., 1998; Kakani et al., 2002; Rodriguez-Enriquez et al., 2013). The uptake of sugars into pollen tubes from the surrounding liquid was proven for tobacco (*Nicotiana tabacum*), *Tradescantia paludosa*, and lily (*Lilium longiflorum*) by measurements with radioactively labeled sugars (Mascarenhas, 1970; Deshusses et al., 1981; Goetz et al., 2017). As pollen tubes are symplastically isolated, sugar uptake across the plasma membrane has to be mediated by transport proteins. Accordingly, it has been shown that at

[1]Current address: Cell Biology, Department of Biology, Friedrich-Alexander University Erlangen-Nuremberg, 91054 Erlangen, Germany.
[2]Address correspondence to ruth.stadler@fau.de.
The author responsible for distribution of materials integral to the findings presented in this article in accordance with the policy described in the Instructions for Authors (www.plantcell.org) is: Ruth Stadler (ruth.stadler@fau.de).
www.plantcell.org/cgi/doi/10.1105/tpc.18.00356

least four sucrose transporters are localized in the plasma membrane of Arabidopsis pollen tubes (Stadler et al., 1999; Meyer et al., 2004; Leydon et al., 2013, 2014; Rottmann et al., 2018a). The additional presence of two cell wall invertases (Hirsche et al., 2009; Ruhlmann et al., 2010) and at least six monosaccharide transporters (Büttner, 2010; Rottmann et al., 2016, 2018b) indicates that besides sucrose, its cleavage products glucose and fructose are also substrates for pollen tubes. Even when considering the high energy demand of pollen tube growth, it seems unlikely that pollen tubes need all those sugar transporters for the uptake of nutrients only. Therefore, it has been discussed that pollen tubes might use sucrose as an osmotically active storage compound that promotes water inflow and pollen tube elongation (Stadler et al., 1999). Furthermore, sugars could serve as signaling molecules for pollen tube growth and/or guidance. It has been shown that numerous processes in plants are influenced by sugars, for example, embryogenesis, germination, seedling development, root and leaf morphogenesis, flowering, stress responses, pathogen defense, wounding responses, and senescence (Sheen et al., 1999; Rolland et al., 2006). Glucose is an especially important signaling molecule that modulates the expression of almost 1000 genes in Arabidopsis via complex regulatory networks (Price et al., 2004; Villadsen and Smith, 2004; Balasubramanian et al., 2007). Among the genes regulated by glucose are those for the monosaccharide transporters STP4 and STP10 (Rottmann et al., 2016), which are localized in pollen tubes.

In this article, we present detailed analyses of the uptake of glucose into pollen tubes of Arabidopsis and of the effects of glucose on pollen tube elongation. In vitro germination assays showed that glucose reduces the growth rate of pollen tubes. In the glucose-insensitive mutant line *hxk1.3*, pollen tubes did not respond to glucose, indicating that glucose acts as a signaling molecule for pollen tube growth and that the glucose sensor HEXOKINASE1 (HXK1) is involved in this regulatory pathway. Measurements with Förster resonance energy transfer (FRET)-based glucose nanosensors revealed that glucose is imported into pollen tubes where it is present in low micromolar concentrations. This is consistent with the $K_m$ values of the monosaccharide transporters of the STP family localized in pollen tubes. Loss of all six transporters led to a reduction of the inhibitory effect of glucose. Reporter gene analyses indicated a strong expression of *HXK1* in pollen tubes. Together with the observation that *hxk1* knockout pollen tubes display an altered growth rate through the pistil, our results point toward an important role of glucose sensing during pollen tube growth or the fertilization process. Potential physiological functions of the glucose inhibition effect are discussed.

## RESULTS

### Analysis of *STP* Expression in Pollen Tubes

The rapid tip growth of pollen tubes consumes a lot of metabolic energy. As pollen tubes are photosynthetically inactive and symplastically isolated, they probably have to take up nutrients from the surrounding tissue. This is underlined by the fact that successful pollen germination in vitro requires the addition of high amounts of sucrose to the germination medium and by the expression of several genes for sucrose transporters in growing pollen tubes (Stadler et al., 1999; Meyer et al., 2004; Qin et al., 2009; Leydon et al., 2013, 2014; Rottmann et al., 2018a). However, microarray data, immunolocalizations, in situ hybridizations, and reporter gene analyses showed that pollen tubes also express several genes for monosaccharide transporters of the STP family (Truernit et al., 1996; Schneidereit et al., 2003, 2005; Scholz-Starke et al., 2003; Wang et al., 2008; Qin et al., 2009; Rottmann et al., 2016, 2018b). RT-PCR analyses confirmed the expression of *STP4*, *STP6*, *STP8*, *STP9*, *STP10*, and *STP11* in pollen tubes (Figure 1A). Because it has been reported for several genes including some members of the *SUC* family that their expression is induced by interaction of the pollen tubes with the maternal tissue, RT-PCR was also performed with cDNAs derived from semi-in vivo cultivated pollen tubes. However, no difference in expression could be observed for the analyzed *STP*s between pollen tubes grown in vitro and semi-in vivo (Figure 1A). With cDNA derived from unpollinated stigmata a PCR product could be obtained only for *STP11* (Figure 1A), indicating that this gene might additionally be expressed in the maternal tissue. All STPs characterized so far have been shown to localize to the plasma membrane. However, for STP4, STP6, STP9, and STP11, this has only been concluded from their ability to mediate glucose uptake across the plasma membrane after heterologous expression of the respective coding sequences in yeast. As subcellular localizations of sugar transporters may differ between yeast and plant cells (Weise et al., 2000; Schneider et al., 2012b), the subcellular localizations of STP4, STP6, and STP9 were verified by expression of the respective coding sequences as fusions to *GFP* in Arabidopsis protoplasts. As shown in Figure 1B, all three fusion proteins clearly labeled the plasma membrane confirming that STP4, STP6, and STP9 are typical plasma membrane localized STPs. The subcellular localization of STP11 was analyzed by transient expression of *LAT52*$_{pro}$*:STP11*c-*GFP* in tobacco pollen tubes. Optical sections of those pollen tubes verified the localization of STP11 in the plasma membrane and additionally showed that the fusion protein is present along the entire pollen tube length (Figure 1C). STP11-GFP was also observed in vesicles at the pollen tube tip, indicating a high protein turnover. These results show that in addition to several sucrose transporters pollen tubes also possess a set of at least six plasma membrane-localized monosaccharide transporters.

### Effect of Glucose on Pollen Germination and Pollen Tube Growth

As glucose is the main substrate of all STPs localized in pollen tubes (Truernit et al., 1996; Schneidereit et al., 2003, 2005; Scholz-Starke et al., 2003; Büttner, 2010; Rottmann et al., 2016, 2018b), the influence of glucose on pollen germination and pollen tube growth in vitro was analyzed by the addition of glucose in different concentrations to the pollen germination medium. To keep the total sugar concentration constant at 250 mM, the concentration of sucrose was reduced in the same extent as glucose was added to the medium. As sucrose and glucose have

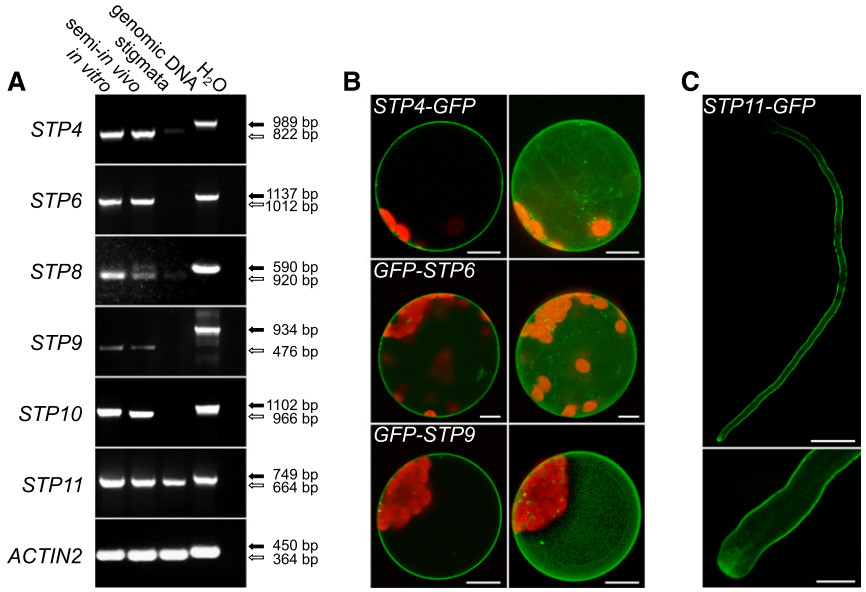


**Figure 1.** Analyses of Pollen Tube-Specific Expression of Different *STP*s and of the Subcellular Localization of the Encoded Proteins.

**(A)** RT-PCR-based comparison of *STP4*, *STP6*, *STP8*, *STP9*, *STP10*, and *STP11* expression in in vitro-germinated pollen tubes, in pollen tubes grown through a stigma (semi-in vivo), and in virgin stigmata with gene-specific primers (Supplemental Table 3). Arrows indicate the predicted sizes of PCR products derived from genomic DNA (black) and reverse-transcribed mRNA (white). The presence of RNA in each sample was confirmed with *ACTIN2* specific primers (Supplemental Table 3).

**(B)** Single optical sections (left) and maximum projections (right) of mesophyll protoplasts expressing *GFP* fusion constructs of *STPs* under the control of the *35S* promoter. GFP is given in green and chlorophyll autofluorescence in red.

**(C)** Confocal optical section of a tobacco pollen tube transiently expressing *STP11-GFP* under the control of $LAT52_{pro}$ after particle bombardment. The bottom image shows the pollen tube tip at higher magnification. Bars = 10 μm in **(B)** and **(C)** (bottom) and 50 μm in **(C)** (top).

comparable osmotic coefficients in this concentration range (Ebrahimi and Sadeghi, 2016), this kept the osmotic pressure of the germination medium constant. To exclude the possibility that the effects on glucose containing media were caused by reduced sucrose concentrations or osmotic effects due to the addition of monosaccharides, additional pollen tube samples were grown on media with less sucrose or with equal concentrations of mannitol, respectively. As shown in Figure 2A, the addition of glucose to the medium slightly reduced the pollen germination rate but only at concentrations ≥75 mM. Moreover, the addition of mannitol seemed to promote pollen germination. By contrast, analyses of pollen tube length revealed that it decreased significantly with increasing glucose concentrations (Figure 2B). This inhibition of pollen tube growth was caused specifically by glucose as neither pollen tubes grown on the respective decreased sucrose concentration nor pollen tubes grown on the same amounts of the sugar alcohol mannitol showed a reduced length (Figure 2B). The specificity of this glucose effect on pollen tube growth was further underlined by the fact that it could not be mimicked by the addition of the enantiomer L-glucose to the growth medium (Figure 2C). The observed decrease in pollen tube length could either be caused by a reduced growth rate or by a shortened growth period. To distinguish between these two possibilities, time series of GFP-labeled pollen tubes growing on medium with or without glucose were acquired and pollen tube growth was analyzed by tracking the movement of their tips (Figure 2D). Under these conditions, growth of pollen tubes ceased on all media ~3 h after the beginning of the experiments, showing that the growth period was not altered by glucose. By contrast, the growth rate was reduced to ~55% in the presence of 50 mM glucose (Figure 2D). This showed that glucose leads to shorter pollen tubes by reducing their growth velocity. The results from the detailed tracking of individual pollen tubes were confirmed by large-scale measurements under the standard conditions used for all other in vitro measurements. To this end the mean length of >200 randomly chosen Col-0 pollen tubes was determined in 1-h intervals from light microscopy images of in vitro grown pollen tubes (Figure 2E). Interestingly, pollen tubes on media with or without glucose elongated at the same rates during the first 3 h (Figure 2E, shaded area). Thereafter, the growth rate of pollen tubes on glucose medium decreased. This effect could still be observed if only the longest 10% of pollen tubes were used for the calculation of the mean value at every time point [Figure 2E, "in vitro (max)"]. Time series in 1-h intervals were also acquired with pollen tubes growing semi-in vivo (Supplemental Figure 1B). During the first 2 h, these pollen tubes elongated inside the stigmatic tissue leading to faster pollen tube growth (Figure 2E, circles). This effect was even more pronounced when pollen tubes were not only grown through the stigma but also through a part of the ovary or even the entire pistil (Supplemental Figure 1A). In contrast to the in vitro cultivation (Figure 2E, triangles), the growth rate under semi-in

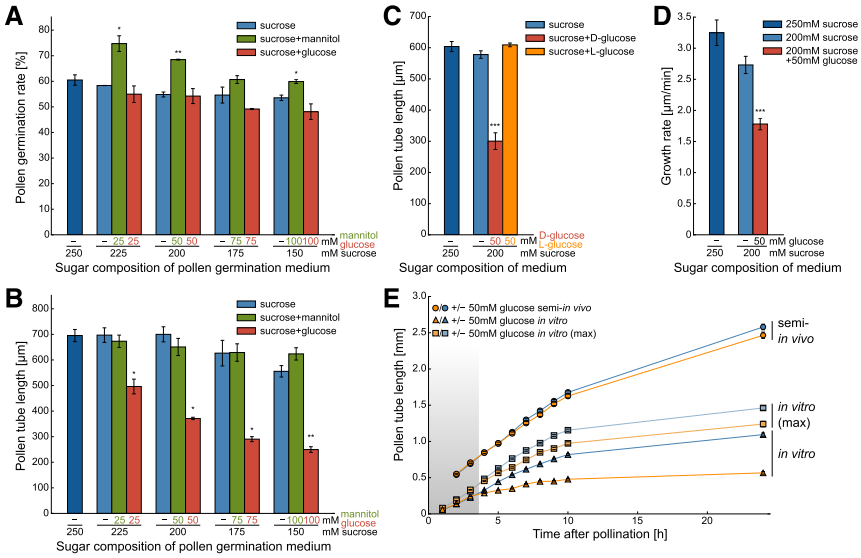


**Figure 2.** Influence of Glucose on Germination and Tube Growth of Col-0 Pollen.

**(A)** In vitro pollen germination rate after 7 h on media with sucrose or sucrose plus different glucose concentrations. Addition of mannitol served as an osmotic control. Bars represent means of three independent experiments ± SE ($n \geq 1500$ in total for every sugar concentration). For this and the following pollen tube growth experiments, "independent experiments" indicates that they were performed on different days with pollen from different plants.
**(B)** Lengths of pollen tubes germinated in vitro for 7 h on media with different sugar concentrations. Mean values ± SE of three biological replicates are shown ($n \geq 600$ in total for every sugar concentration).
**(C)** Lengths of pollen tubes grown in vitro for 7 h on medium supplemented with 50 mM D- or L-glucose. Mean lengths ±SE of five biological replicates ($n \geq 750$ in total for every sugar concentration).
**(D)** Mean growth rate of pollen tubes growing in vitro. Data were obtained by tracking the tip growth of individual pollen tubes in time series taken at intervals of 4 s during hour 1 to hour 3 after spreading pollen on the media ($n = 10$ for every sugar concentration).
**(E)** Comparison of growth rates of pollen tubes germinated in vitro or semi-in vivo on 200 mM sucrose medium with or without additional glucose. Pollen tube lengths were determined every hour. In semi-in vivo experiments only the longest pollen tube of every stigma was measured because it was not possible to measure all lengths due to high pollen tube density (Supplemental Figure 1B). For a better comparability of semi-in vivo and in vitro lengths, the "in vitro (max)" curve is shown, which represents in vitro pollen tube length, when only the longest 10% of pollen tubes were used for the calculation of the mean value at every time point. The shaded area indicates the time during which no influence of glucose on pollen tube growth can be observed under in vitro conditions. Curves show mean values of three independent replicates ± SE [$n \geq 60$ pollen tubes for semi-in vivo and in vitro (max) experiments, $n \geq 600$ for in vitro pollen tubes]. *P ≤ 0.05, **P ≤ 0.01, and ***P ≤ 0.001 by Student's *t* test.

vivo conditions was not reduced on glucose containing medium after the pollen tubes had emerged from the stigma (Figure 2E, circles). This indicates that the growth rate reduction of pollen tubes as a response to glucose is induced during the first hours after pollen germination but manifests only after three hours of growth.

## Contribution of HXK1 to Glucose-Mediated Inhibition of Pollen Tube Growth

The inhibitory effect of glucose makes a function of this sugar as nutrient for pollen tube growth unlikely. However, glucose in plants can serve both as nutrient and as signaling molecule. As HXK1 is a key molecule for glucose signaling in Arabidopsis, the inhibitory effect of glucose on pollen tube growth might be mediated by HXK1. As a first step to test this hypothesis, transgenic *HXK1*$_{pro}$*:HXK1*g-*GFP* and *HXK1*$_{pro}$*:HXK1*g-*GUS* lines were generated to analyze whether *HXK1* is expressed in pollen at all.

Plants driving reporter gene expression from a 3057-bp promoter fragment of *HXK1* were obtained by transformation of Col-0 wild-type plants with the vectors pTR187 (GUS) or pTR188 (GFP). At least 10 independent lines of the resulting BASTA-resistant plants were analyzed. HXK1-GFP was detectable in almost every tissue, for example, in roots (Figures 3B and 3C), sepals (Figure 3D), and ovules (Figure 3E). In all those tissues, HXK1-GFP was localized at mitochondria, which is the reported subcellular localization of HXK1 (Balasubramanian et al., 2007). By far the strongest GFP signal was observed in pollen grains (Figures 3F to 3H and 3L). Expression of *HXK1-GFP* during pollen development became first visible in anthers of stage 9 flowers (Figure 3H) and remained visible until anthesis. During pollen germination, mitochondria with attached HXK1-GFP moved into the outgrowing pollen tube and remained distributed along the entire length of the pollen tube (Figures 3J and 3K). During GUS staining of *HXK1*$_{pro}$*:HXK1*g-*GUS* lines, the blue color first became visible in young lateral roots (Figure 3A) and pollen tubes (Figure 3I), indicating that these are the sites of strongest HXK1 accumulation. The strongest GFP signal originated from mature pollen (Figure 3L). Determination of *HXK1* expression levels in different tissues by RT-qPCR revealed low expression of *HXK1*

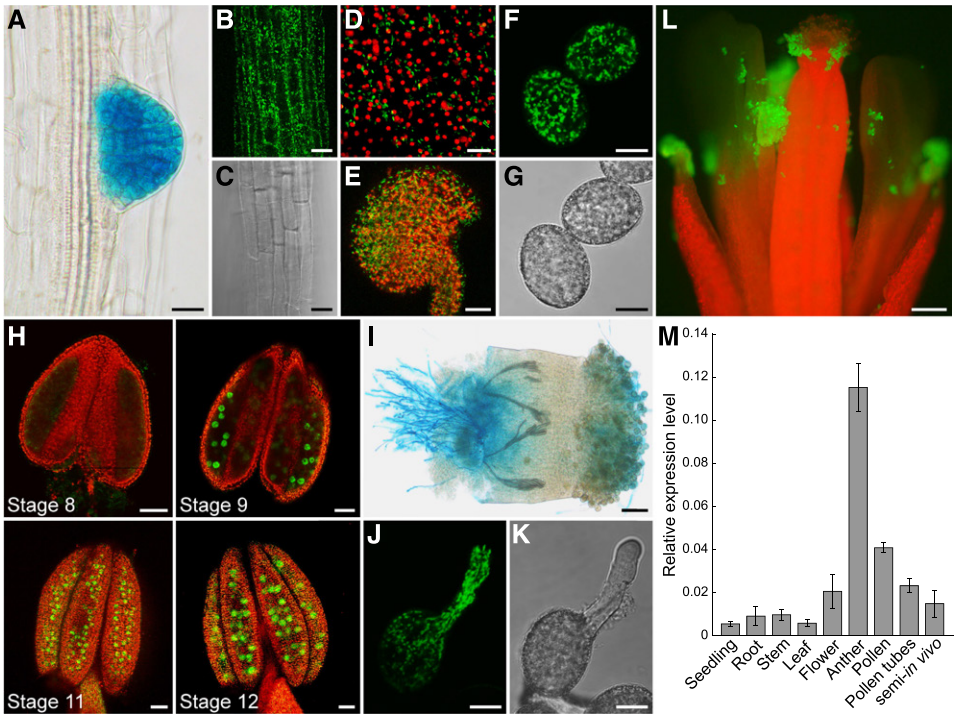


**Figure 3.** Analyses of *HXK1* Expression in Different Tissues by Reporter Plant Studies and RT-qPCR.

**(A)** and **(I)** Histochemical detection of GUS activity in Arabidopsis Col-0 expressing an *HXK1*$_{pro}$:*HXK1*g-*GUS* construct.
**(B)** to **(H)** and **(J)** to **(L)** Detection of GFP fluorescence (green) by confocal microscopy in *HXK1*$_{pro}$:*HXK1*g-*GFP* reporter plants. Chlorophyll autofluorescence is given in red.
**(A)** Root of an 8-d-old seedling with strong GUS staining in an emerging lateral root.
**(B)** Root epidermis cells with HXK1-GFP.
**(C)** Bright field of **(B)**.
**(D)** Epidermal cells of a sepal.
**(E)** Maximum projection of an excised ovule.
**(F)** Mature pollen grains with HXK1-GFP at the mitochondria.
**(G)** Bright field of **(F)**.
**(H)** Anthers of different floral stages with HXK1-GFP in developing pollen grains. All flower stages 1 to 20 were named according to Smyth et al. (1990).
**(I)** Pollen tubes grown semi-in vivo on a wild-type stigma.
**(J)** In vitro growing pollen tube.
**(K)** Bright field of **(J)**.
**(L)** Open pollinated flower. Bars = 20 μm in **(A)** to **(C)** and **(E)**, 10 μm in **(D)**, **(F)**, **(G)**, **(J)**, and **(K)**, 50 μm in **(H)** and **(I)**, and 200 μm in **(L)**.
**(M)** Analysis of *HXK1* transcript levels in different tissues. *HXK1* transcripts were quantified by RT-qPCR using total RNA extracted from seedlings, roots, stems, leaves, pollinated flowers, young anthers, mature pollen, in vitro-germinated pollen tubes, and pollen tubes grown semi-in vivo through stigmata. The diagram depicts expression ratios relative to *UBI10* expression in each tissue. Bars represent mean values ± SE of three biological replicates with three technical replicates each. For each biological replicate, the tissue for RNA isolation was collected from a different Col-0 plant.

in almost all tissues tested (Figure 3M). The only exception was young anthers with developing pollen that showed almost a 5- to 10-fold higher expression of *HXK1* compared with other tissues (Figure 3M). In contrast to the data obtained by reporter gene analysis, *HXK1* expression was quite low in mature pollen and in pollen tubes. As the reporter plants provide information about the accumulated protein, this indicated that *HXK1* is mainly expressed during pollen development and that the accumulated protein is stable during pollen germination and tube growth.

The prominent accumulation of HXK1 in pollen tubes suggests that this glucose sensor might be involved in the glucose-mediated inhibition of pollen tube growth. To analyze this further, pollen of *hxk1* mutant lines were germinated in vitro on media with or without glucose. Pollen tube growth of the mutant line *gin2-1* (*glucose insensitive2-1*) that carries a premature stop codon in the *HXK1* gene was not reduced on medium with glucose (even at high concentrations) and pollen tubes were even longer on glucose-free medium compared with the wild type (Figure 4A). The *gin2-1* mutation is in the L*er* background, but the respective L*er* wild-type pollen showed the same glucose-dependent growth inhibition as Col-0 pollen. The pollen tube growth assay was repeated with a T-DNA insertion line of *HXK1* in the Col-0 background, which was named *hxk1.3.* Two other potential lines (*hxk1.1* [SALK_015782] and *hxk1.2* [SALK_018182]) had

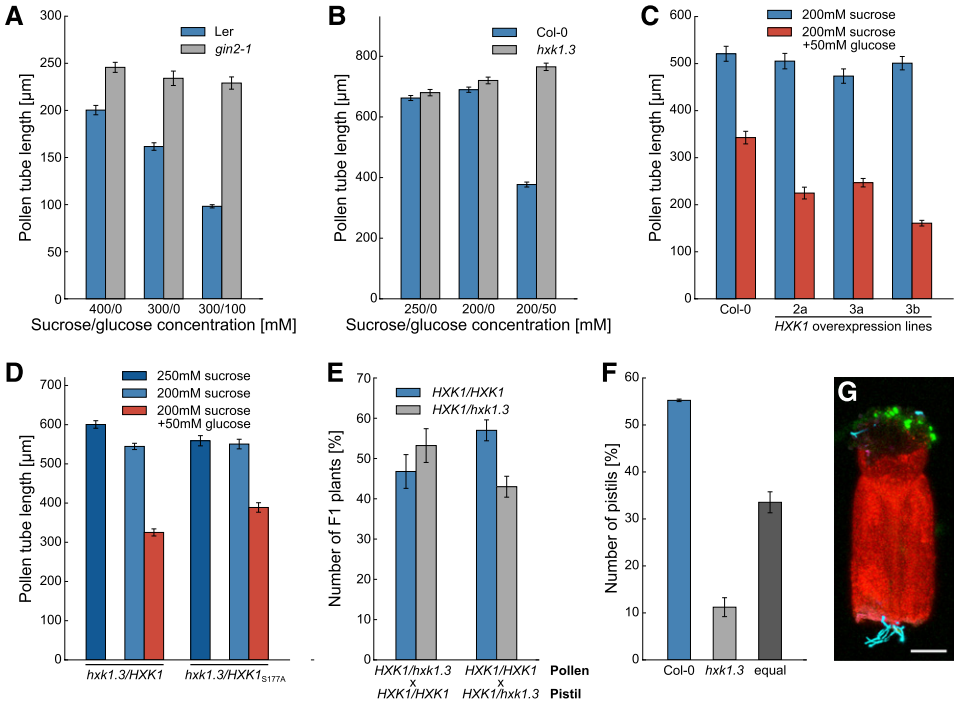


**Figure 4.** Characterization of the Glucose-Insensitive Mutants *gin2-1* and *hxk1.3* Regarding Pollen Tube Growth.

**(A)** Mean lengths ± SE of *gin2-1* and wild-type (Ler) pollen tubes grown in vitro for 7 h on media with or without glucose ($n \geq 200$ for every genotype on every sugar concentration).

**(B)** Lengths of *hxk1.3* and wild-type (Col-0) pollen tubes grown in vitro for 7 h on media with or without glucose. Mean values of three independent experiments ± SE are shown ($n \geq 600$ in total for every mean value). Independent experiments were performed on different days with pollen from different plants.

**(C)** In vitro pollen tube lengths of three independent *HXK1* overexpression lines in comparison to wild-type (Col-0) on media with or without glucose ($n \geq 200$ pollen tubes for each line).

**(D)** Pollen tube lengths of *hxk1.3* complementation lines on medium with or without glucose. Complementation lines were generated by transformation of homozygous *hxk1.3* plants with *LAT52*$_{pro}$*:HXK1*c or with *LAT52*$_{pro}$*:HXK1*c$_{S177A}$ encoding a catalytically inactive form of HXK1. Bars represent means of three biological replicates ± SE ($n \geq 370$ for every mean value).

**(E)** Genotypes regarding *HXK1* in the F1 descendants of cross-pollination experiments with heterozygous *hxk1.3*/*HXK1* pollen and pistils from Col-0 plants. Reciprocal crosses were performed with Col-0 pollen and heterozygous *hxk1.3*/*HXK1* pistils. Bars represent mean values of the percentage of each genotype in the F1 generation of four independent crossings (four different plants were used for crossing; $n \geq 98$ F1 seedlings in total).

**(F)** Results of the "pollen-tube race" experiment. Col-0 pistils were pollinated with GFP-labeled *hxk1.3* pollen and Col-0 pollen expressing *TagRFP-T*, cut in the middle, and placed horizontally on germination medium. The graph depicts which pollen tubes emerged first form the cut-surface. Mean values ± SE of three independent replicates (pollen and pistils of different plants were used on three different days) with 70 stigmata in total.

**(G)** Representative confocal image of a "pollen-tube race" experiment. GFP is given in green, TagRFP-T in cyan, and chlorophyll autofluorescence in red. Bar = 150 µm.

no detectable T-DNA insertion. On medium without glucose *hxk1.3* pollen tubes did not show any difference compared with wild-type pollen tubes, but whereas growth of wild-type pollen tubes was inhibited on glucose containing medium, *hxk1.3* pollen tubes reached the same length as on glucose-free medium (Figure 4B). This clearly showed that glucose inhibits pollen tube growth via an HXK1-dependent pathway, and glucose therefore seems to be a signaling molecule for pollen tubes. For further analyses, *hxk1.3* was used as glucose-insensitive mutant line because the Col-0 background provided better comparability to other experiments as all other mutants used in this study were also derived from this ecotype. The transformation of homozygous *hxk1.3* plants with the construct *LAT52*$_{pro}$*:HXK1*c complemented the phenotype and pollen tubes of the complementation lines were again sensitive to glucose (Figure 4D). This complementation also worked with the construct *LAT52*$_{pro}$*:HXK1*c$_{S177A}$ (Figure 4D), which encodes a catalytically inactive form of HXK1 (Cho et al., 2006), indicating that the kinase function of HXK1 is not necessary for its role as glucose sensor in pollen tubes. The role of HXK1 as glucose sensor in pollen tubes was underlined by the fact that pollen tubes overexpressing *HXK1* were hypersensitive to glucose and produced shorter pollen tubes than did the wild type on glucose-containing medium (Figure 4C). To analyze the influence of HXK1 on pollen tube growth in vivo, a cross-pollination experiment was performed by pollinating Col-0 pistils with pollen of heterozygous *hxk1.3*/*HXK1*

plants. After meiosis in a heterozygous plant, 50% of the haploid pollen carry the *hxk1.3* allele and 50% have the wild-type allele. If the mutation has no impact on the ability of the pollen tubes to fertilize the ovules, half of the ovules should be fertilized by wild-type pollen tubes and the other half by mutant pollen tubes. As a result, 50% of the F1 descendants should inherit the mutant allele and the other half the wild-type allele. However, even small changes in the ability of the mutant pollen tubes to fertilize the ovule would result in an altered competition between wild-type and mutant pollen tubes, which then would manifest in the ratio of wild-type to mutant alleles in the F1 generation. The observed segregation ratio of homozygous:heterozygous plants in the F1 generation did not differ greatly from the 50:50 ratio expected for mendelian segregation (Figure 4E), indicating that the ability to sense glucose was not essential for pollen fertility under the given conditions. Also, reciprocal crossings with heterozygous *hxk1.3*/*HXK1* pistils and Col-0 pollen resulted in a normal segregation ratio in the descendant generation (Figure 4E). When *hxk1.3* pollen tubes labeled with GFP and TagRFP-T-labeled wild-type pollen tubes were grown simultaneously semi-in vivo through a half pistil, only in 11% of the experiments were *hxk1.3* pollen tubes the first to emerge from the cut surface (Figures 4F and 4G). The result of this "pollen tube race" experiment indicated that glucose sensing by pollen tubes is necessary for their growth through the transmitting tract under certain conditions. Cutting the pistil for the race experiment led to wounding of the tissue, which represents a stress applied to the plants. As no reduced fertility of *hxk1.3* pollen in direct comparison to wild-type pollen was observed in the cross-pollination experiment, this indicated that glucose sensing might only play a role during stress conditions. Taken together, the pollen tube phenotypes of *hxk1* mutants in vitro and in vivo indicated that glucose-mediated inhibition of pollen tubes is mediated via HXK1 and that the ability to sense glucose influences pollen tube growth in the pistil under certain conditions.

### Detection of Glucose Uptake into Pollen Tubes with Cytosolic FRET Glucose Sensors

The dependence of the glucose-induced inhibition of pollen tube growth on the cytosolic glucose sensor HXK1 prompted us to wonder how much glucose is taken up from the medium into the cells. To analyze this, stable Arabidopsis lines expressing different *FLIP*glu constructs under the control of the pollen-specific promoter $LAT52_{pro}$ were generated. FLIPglus are FRET-based glucose nanosensors consisting of the FRET donor eCFP coupled to the FRET acceptor eYFP via a glucose binding protein (Figure 5A). Binding of glucose to the glucose binding protein leads to conformational changes that increase the distance between eCFP and eYFP and thus to a disruption of FRET. Quantification of the FRET efficiency therefore allows the visualization of alterations in glucose concentrations in living cells. Point mutations in the glucose binding protein led to several FLIPglu variants with different affinities for glucose (Deuschle et al., 2006) that were all used for glucose uptake measurements in pollen tubes. FLIPglu pollen tubes were grown semi-in vivo together with donor only and acceptor only control pollen tubes in a perfusion chamber filled with liquid pollen germination medium containing 250 mM sucrose (Supplemental Figure 2). During time-series recordings, pollen tubes were

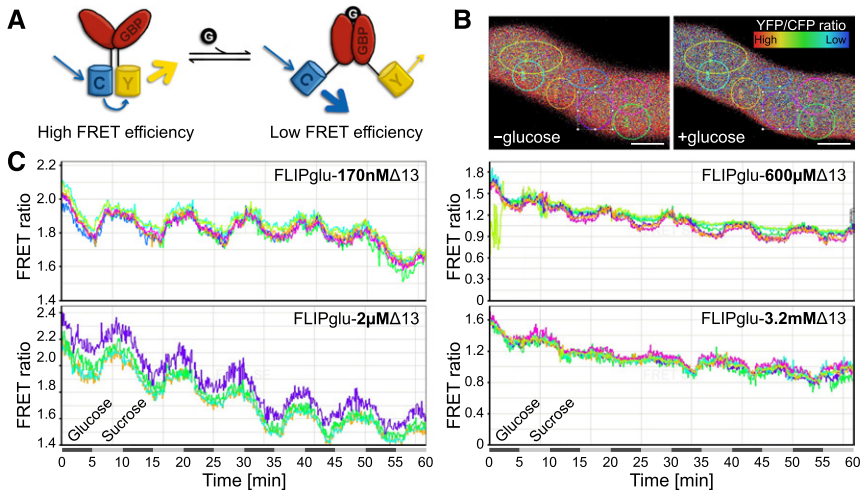


**Figure 5.** Uptake of Glucose into Pollen Tubes Detected with FRET-Based Glucose Nanosensors.

**(A)** Scheme of FLIPglu nanosensor function. eCFP (C) and eYFP (Y) are linked via a glucose binding protein (GBP). The conformational change upon binding of glucose to the GBP increases the distance between the chromophores and FRET efficiency decreases.

**(B)** Ratiometric images of the same pollen tube in the presence and absence of glucose. Colored circles represent ROIs used for FRET ratio calculation. Bar = 2.5 μm.

**(C)** Response of pollen tubes from transformants expressing *FLIP*glu-170nΔ13, *FLIP*glu-2μΔ13, *FLIP*glu-600μΔ13, or *FLIP*glu-3.2mΔ13 to perfusion with 50 mM glucose. Sugar concentration in the medium was changed between 250 mM sucrose and 200 mM sucrose + 50 mM glucose in intervals of 5 min. Quantification of FRET ratio was performed using the Leica FRET Sensitized Emission Wizard application.

constantly perfused with liquid medium. Sugar concentration in the medium was changed between 250 mM sucrose and 200 mM sucrose + 50 mM glucose every 5 min, and FRET responses were observed on the same specimen for 1 h. Pollen tubes with FLIPglu-170nΔ13 responded to glucose perfusion with a decrease of FRET efficiency (Figures 5B and 5C), indicating that glucose was taken up into the pollen tube and that uptake was faster than metabolism and compartmentation. In ~4 to 5 min after glucose withdrawal, the FRET ratio returned almost to the initial value, suggesting that the imported glucose was rapidly metabolized or removed from the cytosol. Analyses with FLIPglu-2μΔ13 also gave consistent results with a reduction of FRET ratio upon glucose supply (Figure 5C). By contrast, pollen tubes containing FLIPs with lower glucose affinities (FLIPglu-600μΔ13 or FLIPglu-3.2mΔ13) showed almost no response to added glucose. The fact that glucose alterations in pollen tubes could be monitored with the high-affinity nanosensors but not with FLIPglu-600μΔ13 or FLIPglu-3.2mΔ13 indicates that the steady state glucose levels in the cytosol of pollen tubes lie within the detection range of FLIPglu-170nΔ13 (0.019–1.53 μM; Fehr et al., 2003) and FLIPglu-2μΔ13 (0.2–20 μM; (Chaudhuri et al., 2011) and, thus, in the low micromolar range.

### Role of STP Uptake Activity in Pollen Tube Growth Inhibition

The changes in cytosolic glucose concentrations observed by FRET measurements lie in the same range as the $K_m$ values for glucose uptake of the pollen tube-specific STPs (Truernit et al., 1996; Schneidereit et al., 2003, 2005; Scholz-Starke et al., 2003; Büttner, 2010; Rottmann et al., 2016, 2018b). To study the contribution of STPs to glucose uptake into growing pollen tubes, knockout lines of all *STP*s detected in pollen tubes were analyzed with regard to pollen tube growth. New T-DNA insertion lines for *STP6*, *STP9*, and *STP11* were ordered and characterized. Sequencing of the mutant alleles identified the T-DNA insertions of *stp6.1* and *stp9.1* in exon regions 355 and 1158 bp after the start codon, respectively (Supplemental Figure 3A). The T-DNA in *stp11.1* is inserted only 62 bp upstream of the stop codon and truncated transcripts could still be detected in homozygous plants (Supplemental Figure 3C). Therefore, we used *stp11.2* with an insertion in the middle of the second exon (Supplemental Figure 3A). Homozygous plants of *stp6.1*, *stp9.1*, and *stp11.2* (Supplemental Figure 3B) had no full-length transcripts of the respective genes (Supplemental Figure 3C), indicating that they are complete knockout lines. In contrast to all other characterized *stp* knockout lines, which are derived from Col-0, *stp11.2* was in the L*er* background. For better comparability, *stp11.2* was crossed back into Col-0 five times before phenotypic analysis.

Unfortunately, no T-DNA line with an insertion in the coding sequence of *STP4* was available. Therefore, Col-0 plants were transformed with the plasmid pFC18 that contained the *Cas9* gene and the sequence for a single-stranded guide RNA (sgRNA) targeting *STP4*. In the F1 generation of all BASTA-resistant plants, *Cas9* could be detected by PCR (Figure 6B). After self-fertilization, plants of the F2 generation that had lost *Cas9* by segregation were identified by PCR (Figure 6B) and tested for mutations in *STP4* by sequencing.

Plants of line #1.1 had lost *Cas9* and carried a heterozygous deletion of 4 bp directly upstream of the *PAM* sequence, which leads to a frameshift and a premature stop codon in *STP4* (Figure 6A). Among the descendants of line #1.1 plants homozygous for the deletion were identified that are referred to as knockout line *stp4.1*. Homozygous plants of line *stp4.1* as well as *stp6.1*, *stp8.1* (Rottmann et al., 2018b), *stp9.1*, *stp10.1* (Rottmann et al., 2016), and *stp11.2* were used for pollen germination assays on media with or without glucose. Whereas the mean pollen tube lengths of all *stp* knockout lines were comparable to the wild type on medium with sucrose only, all mutant lines had slightly longer pollen tubes on 50 mM glucose (Figure 7A). This indicated that the knockout of one *STP* led to a weak reduction

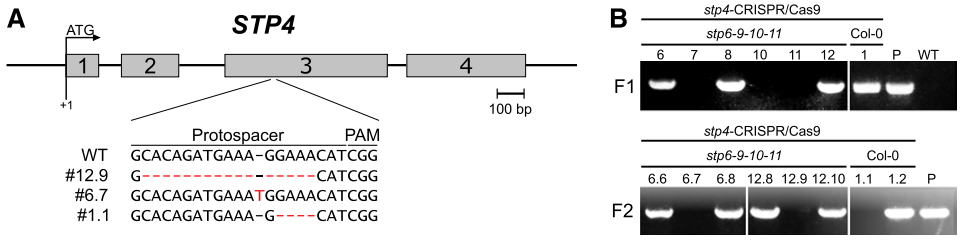


**Figure 6.** Generation of *stp4* Knockout Lines by CRISPR/Cas9-Mediated Mutagenesis.

**(A)** Genomic organization of *STP4*. Exon regions (gray bars) are numbered; introns and untranslated regions are shown as black lines. The positions of the protospacer sequence and the mutations identified in plants transformed with the *CRISPR/Cas9* construct are indicated. The plant lines were named #x.y, with x representing the number of the plant selected in the F1 generation and y offspring plant chosen in the respective F2 generation.
**(B)** Control PCRs performed during generation of *stp4* knockout lines by CRISPR/Cas9. In the F1 generation after dipping of Col-0 or stp6-9-10-11 plants, the presence of *Cas9* was confirmed by PCR with the primer pair listed in Supplemental Table 2. The image shows representative results for plants 6, 7, 8, 10, 11, and 12 in the *stp6-9-10-11* background and plant 1 in the Col-0 background of 20 plants tested. The plasmid used for transformation was used as a positive control (P), and genomic DNA isolated from a wild-type plant (WT) served as negative control. Plants of the F2 generation that had lost *Cas9* by segregation were identified by PCR with the same primers as used before and analyzed for changes in *STP4* by sequencing. The plant lines were named #x.y, with x representing the number of the plant selected in the F1 generation and y offspring plant chosen in the respective F2 generation.

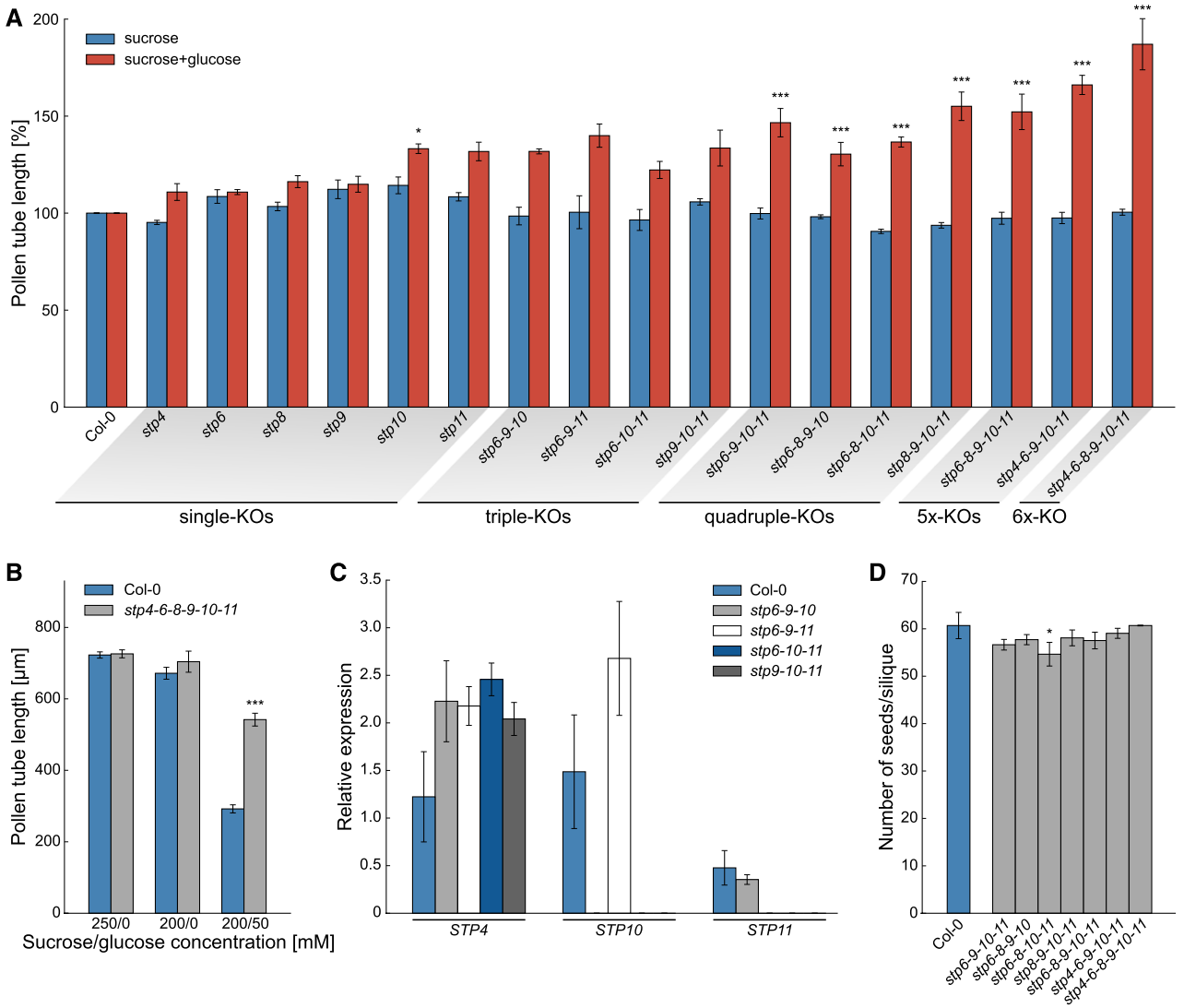


**Figure 7.** Analysis of Single and Multiple Knockout Lines of Pollen Tube-Expressed *STP*s.

**(A)** Pollen tube lengths of *stp* single, triple, quadruple, quintuple, and sextuple knockouts. Pollen tubes were grown for 7 h in vitro on medium with 250 mM sucrose or 200 mM sucrose + 50 mM glucose. Bars represent mean values of three individual replicates ± SE ($n \geq 420$ pollen tubes for each mean value). For each biological replicate, flowers of different plants of the same genotype were used for pollen sampling. During each mutant pollen germination experiment, pollen of a wild-type plant cultivated under the same conditions was germinated in parallel. For better comparability of the different knockout lines, pollen tube lengths of mutants are given as relative values compared with the mean pollen tube length of the respective wild type on the same medium. Statistical analysis was performed prior to this normalization step.
**(B)** Mean lengths ±SE of *stp4-6-8-9-10-11* sextuple knockout and wild-type (Col-0) pollen tubes grown in vitro for 7 h on medium with or without glucose ($n \geq 550$ pollen tubes for every genotype on every sugar concentration in three independent replicates).
**(C)** Analyses of *STP4*, *STP10*, and *STP11* transcript levels in pollen tubes of Col-0 and different *stp* triple knockout lines. Transcripts were quantified by RT-qPCR with primers listed in Supplemental Table 5 using total RNA extracted from Col-0 or mutant pollen tubes grown in vitro for 7 h. The diagram depicts expression ratios relative to *UBI10*. Means of three biological replicates (with three technical replicates each) ± SE are shown. For every biological replicate, pollen of four different flowers from individual plants was used for pollen germination and subsequent RNA isolation.
**(D)** Average number of seeds/silique ± SD of multiple *stp* knockout plants and wild-type plants after self-pollination. $n > 30$ siliques/genotype. *P ≤ 0.05 and ***P ≤ 0.001 by Student's *t* test.

in glucose uptake and as a result to a decrease of the glucose inhibition effect. However, the phenotype was only marginal, probably due to functional redundancy of the remaining STPs that can still mediate glucose uptake into pollen tubes. Therefore, multiple knockouts of pollen tube expressed *STP*s were generated by crossings of the single mutants. However, even the knockout of three *STP*s increased the insensitivity toward glucose only slightly compared with the single knockout lines (Figure 7A). RT-qPCR analysis of mRNA derived from pollen tubes revealed that some of the remaining *STP*s are upregulated in *stp* triple knockout lines (Figure 7C), offering an explanation for the weak phenotype. Therefore, higher-order mutant lines were generated by crossing different triple knockout lines. Different combinations of *stp* quadruple mutations and the *stp6-8-9-10-11* and *stp4-6-9-10-11* quintuple knockout lines indeed showed significantly increased pollen tube lengths on glucose medium compared with the wild type (Figure 7A). However, even the pollen tubes of *stp6-8-9-10-11* plants still showed a strong growth reduction in the presence of glucose and like the quadruple knockouts produced normal amounts of seeds (Figure 7D). Generation of *stp4-6-8-9-10-11* sextuple knockout lines was started by transformation of *stp6-9-10-11* mutants with pFC18 as the *stp8.1* allele already conveys BASTA resistance. Two lines of the F2 generation that had lost *Cas9* by segregation (Figure 6B) showed indels in the *STP4* sequence. The insertion of 1 bp in line #6.7 and the deletion of 16 bp in line #12.9 (Figure 6A) both led to frameshift mutations, and plants heterozygous for these alleles were crossed with homozygous *stp6-8-9-10-11* mutants. Genotyping of F2 seedlings after crossing led to the identification of sextuple knockouts with mutations in *STP4*, *STP6*, *STP8*, *STP9*, *STP10*, and *STP11*. These sextuple knockout plants showed normal vegetative growth and formed pollen tubes as long as those in wild-type plants on medium with 250 mM sucrose (Figure 7A). However, on glucose-containing medium, pollen tubes defective in six STPs reached the double length of wild-type pollen tubes (Figure 7A) and their growth was only slightly reduced compared with those cultured on medium without glucose (Figure 7B). This indicates that glucose is indeed taken up into pollen tubes via the pollen tube localized monosaccharide transporters STP4, STP6, STP8, STP9, STP10, and STP11 in an additive manner.

### Influence of Fructose on Glucose-Mediated Pollen Tube Growth Inhibition

qPCR analyses in a previous study revealed that the expression of *STP4* and *STP10* is downregulated in pollen tubes grown in vitro on medium with glucose probably via HXK1 (Rottmann et al., 2016). However, glucose-dependent downregulation was absent when fructose was added to the medium in equimolar amounts. The same regulation of gene expression in pollen tubes by the addition of glucose and fructose to the medium was observed for *STP8* (Figure 8A). Length measurements of pollen tubes revealed that fructose alone has no influence on pollen tube growth (Figure 8C). However, when fructose was added to medium that contained growth-inhibiting glucose, pollen tubes reached the same lengths as on medium without the monosaccharide (Figure 8B), indicating that fructose is able to suppress the inhibitory effect of glucose. This neutralizing effect of fructose was concentration dependent peaking at equimolar amounts of fructose to glucose (Figure 8B). As fructose sensing in roots is mediated by FINS1/FBP (Cho and Yoo, 2011) the same experiment was repeated with pollen of homozygous *fins1* knockout plants to test whether FINS1/FBP is also involved in the observed fructose effect on pollen tube growth. However, fructose also neutralized the glucose-induced pollen tube inhibition of *fins1* pollen (Figure 8C), indicating that FINS1/FBP in this context is not required for fructose sensing in pollen tubes. Another hypothesis was that fructose might inhibit glucose uptake by interfering with its transport by STPs. However, as an excess of fructose did not reduce the uptake of $^{14}$C-glucose into yeast strains expressing several of the pollen tube-specific *STP*s (Figure 8D) this hypothesis was disproved.

### Potential Contribution of SWEETs to Extracellular Sugar Concentrations in the Pistil

Sucrose can be unloaded from the phloem into cells of the pistil symplastically (Werner et al., 2011). It has been suggested that sucrose is then exported into the apoplast of the transmitting tract where it serves as nutrient for the growing pollen tubes. As the cleavage of sucrose by cell wall invertases leads to equimolar amounts of fructose and glucose, glucose derived from sucrose would not be interpreted as a signal for the reduction of growth rates by pollen tubes. Therefore, the question arose as to how additional glucose that functions as a signal molecule might be provided. Potential candidates were glucose-specific SWEET carriers that can release additional glucose into the apoplast. Microarray data suggested a high expression of *SWEET1*, *SWEET9*, and *SWEET10* in pistil tissues (Swanson et al., 2005). These genes encode glucose- (SWEET1; Chen et al., 2010) and sucrose-specific (SWEET9 [Lin et al., 2014] and SWEET10 [Chen et al., 2012]) transporters. To further analyze the expression patterns of these *SWEETs*, transgenic *SWEET*$_{pro}$*:SWEET*g-*GUS* Arabidopsis plants were generated. Plants driving *SWEET1*g-*GUS* expression from an 1810-bp *SWEET1* promoter fragment showed a weak blue staining in anthers (Figure 9A). The pistil showed GUS activity only in the style (Figures 9A and 9B). In this tissue, promoter activity was very strong and, therefore, also the adjacent stigmatic tissue appeared blue after prolonged incubation (Figure 9A). However, papillar cells did not show GUS activity in any of the five lines analyzed. Cross sections of stained pistils revealed that *SWEET1* is expressed mainly in the vascular tissue of the pistil but also in cells of the transmitting tract (Figure 9C). GUS staining of plants expressing *SWEET9*g-*GUS* under the control of a 1359-bp fragment of the *SWEET9* promoter led to a blue staining of the stigmatic papillae (Figures 9D and 9E) and also showed the already described expression of *SWEET9* in nectaries (Lin et al., 2014). In flowers of *SWEET10*$_{pro}$*:SWEET10*g-*GUS* plants, GUS staining was observed in anthers and along the vascular tissue of the pistil especially in the stylar region (Figures 9F and 9G). The observed expression patterns of these genes in flowers indicate that SWEET9 and SWEET10 could supply the germinating pollen and growing pollen tubes with sucrose, whereas SWEET1

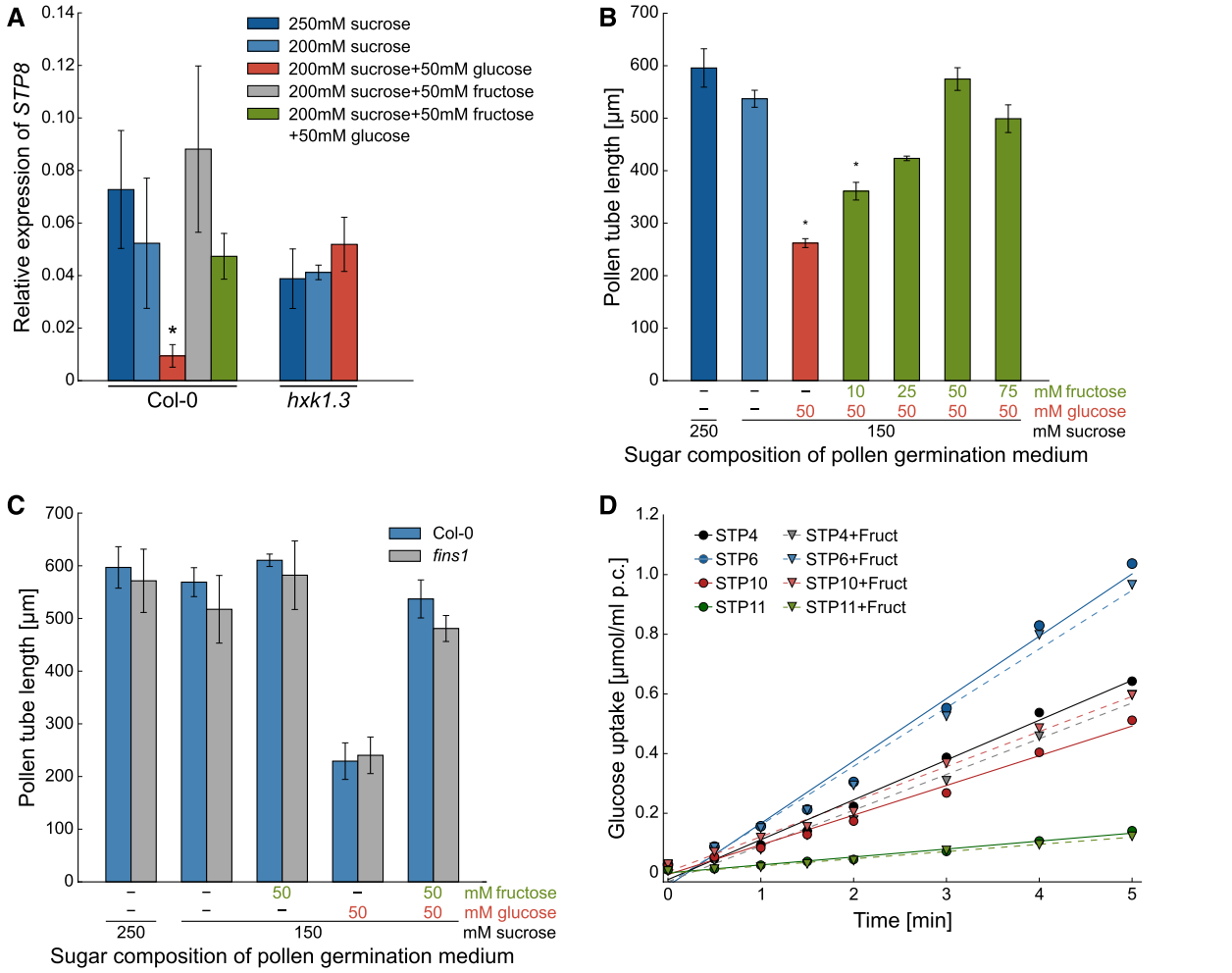


**Figure 8.** Influence of Fructose on Expression of *STP8*, Pollen Tube Growth, and Glucose Uptake via STPs.

**(A)** Analysis of *STP8* transcript levels in Col-0 and *hxk1.3* pollen tubes germinated in vitro on media with different sugars. *STP8* transcripts were quantified by RT-qPCR using total RNA extracted from Col-0 or *hxk1.3* pollen tubes grown in vitro for 6 h on media containing either 250 mM sucrose, 200 mM sucrose, or 200 mM sucrose supplemented with 50 mM of glucose, fructose, or glucose and fructose. The diagram depicts expression ratios relative to *UBI10* expression under each growth condition. Bars represent mean values of three biological replicates with three technical replicates each. For every biological replicate, pollen of four different flowers from individual plants was used for pollen germination and subsequent RNA isolation. Error bars correspond to SE. *P ≤ 0.05 by Student's *t* test.

**(B)** Lengths of Col-0 pollen tubes on medium with sucrose only, sucrose with glucose, or sucrose with glucose and different concentrations of fructose. Lengths were measured 7 h after germination. Means of three biological replicates ± SE are shown ($n \geq 570$ pollen tubes in total for every medium composition). Biological replicates were produced by usage of pollen from different plants on different days. *P ≤ 0.05 by Student's *t* test.

**(C)** Mean lengths ± SE of *fins1* and Col-0 pollen tubes grown in vitro for 7 h on medium supplemented with glucose, fructose, or glucose and fructose ($n \geq 200$ pollen tubes for every genotype on every sugar concentration).

**(D)** Determination of $^{14}$C-glucose transport activity of STP4, STP9, STP10, and STP11 in the presence of nonradioactive fructose in 10-fold excess. Uptake of $^{14}$C-glucose into yeast cells expressing *STP4*, *STP9*, *STP10*, or *STP11* was determined at an initial outside concentration of 20 µM at pH 5.5.

could contribute to the release of glucose into the apoplast of the pistil where it could serve as a signal for pollen tubes.

### Physiological Relevance of the Glucose-Induced Inhibition of Pollen Tube Growth

The HXK1 dependence of the glucose-induced growth inhibition of pollen tubes and the reduced growth of *hxk1.3* pollen tubes in the pollen tube race experiment indicate that glucose is an important signal for pollen tube growth in the pistil. Several theories on the physiological function of glucose inhibition have been tested. A possible function of glucose as pollen tube guidance signal has been ruled out by analyses of pollen tube growth direction on media with internal glucose gradients or by placing glucose containing gelatin beads in front of growing pollen tubes. In none of the experiments did pollen

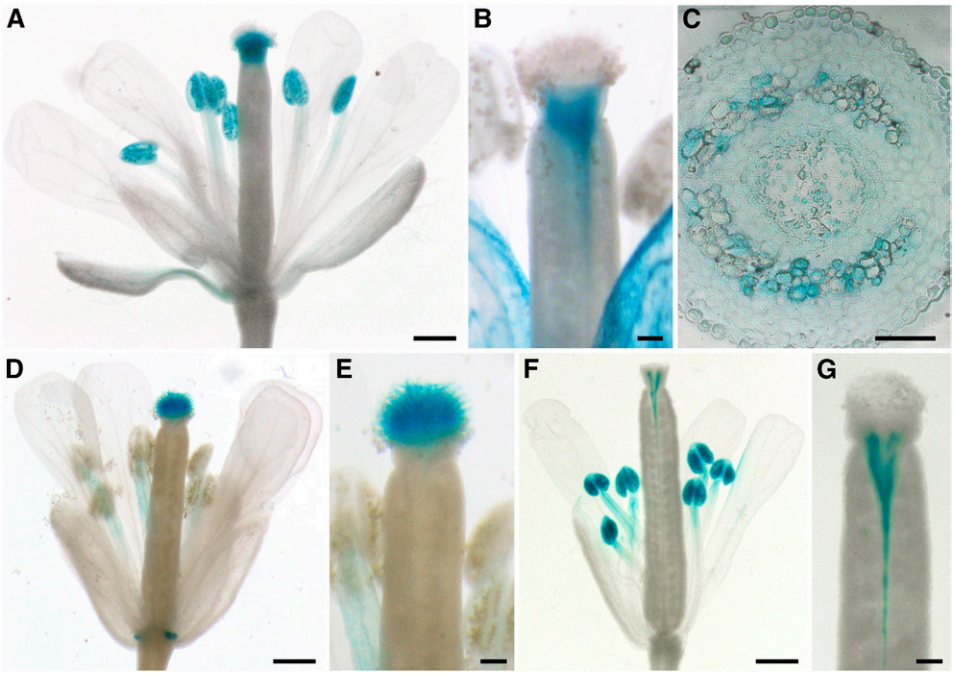


**Figure 9.** Analyses of *SWEET1*, *SWEET9*, and *SWEET10* Expression in Pistils.

**(A)** to **(C)** Histochemical detection of β-glucuronidase activity in flowers of Arabidopsis Col-0 expressing a *SWEET1*$_{pro}$:*SWEET1*g-*GUS* fusion construct.
**(A)** Pollinated stage-14 flower with strong GUS signals in the anthers and the stigma.
**(B)** Stigma at higher magnification stained for a shorter time compared with **(A)** to better see the origin of GUS staining in the region of the style.
**(C)** Cross section through the style of a GUS-stained pistil.
**(D)** and **(E)** Detection of GUS activity in Col-0 plants transformed with a *SWEET9*$_{pro}$:*SWEET9*g-*GUS* construct.
**(D)** Flower with GUS staining in the stigma and the nectaries.
**(E)** Stigma at higher magnification.
**(F)** and **(G)** Histochemical detection of GUS activity in flowers of Arabidopsis Col-0 expressing a *SWEET10*$_{pro}$:*SWEET10*g-*GUS* fusion construct.
**(F)** Flower with GUS staining in the anthers and near the vascular tissue.
**(G)** Upper part of the ovary at higher magnification.
Bars = 500 μm in **(A)**, **(D)**, and **(F)**, 100 μm in **(B)**, **(E)**, and **(G)**, and 50 μm in **(C)**.

tubes show a change in growth direction as a response to glucose (Figures 10A to 10C). It is well known that many plants produce fewer seeds under stress conditions. For temperature stress, it has been reported that the reduced seed set is often caused by reduced pollen fertility and pollen tube growth (Zinn et al., 2010). The inhibitory effect of glucose on pollen tube growth suggested that an increased glucose concentration in the transmitting tract might be responsible for the reduced fertility of Arabidopsis under temperature stress. However, when the numbers of seeds produced by Col-0, *hxk1.3*, and *HXK1-OE* plants after heat stress treatment were compared, no differences were observed between the wild type and mutants (Figure 10D). The reduced seed set of all three plant lines under heat stress showed that this effect is independent of HXK1 and, therefore, is probably not mediated by glucose-induced inhibition of pollen tube growth. Reduced pollen tube growth has also been described in connection with the so called "pollen population effect" (Ter-Avanesian, 1978; Holm, 1994). It has been observed that a low pollination density leads to reduced germination and shorter pollen tubes, whereas high pollen density promotes germination and tube growth. To test whether this effect is mediated by glucose, different amounts of pollen from wild-type and *hxk1.3* mutants were germinated in vitro. Pollen length measurements revealed that the population effect was even more severe on medium with glucose (Figure 10E). However, there was no difference between Col-0 and *hxk1.3* pollen tubes, indicating that also the population effect is not mediated by HXK1. A screen for glucose sensitivity of pollen tubes of several plant species revealed that only a few taxa within the Brassicaceae show a glucose-induced inhibition of pollen tube growth (Figure 11). The evenly distributed formation of seeds in a silique requires a tightly controlled targeting of pollen tubes to each ovule in the ovary. A slowing down of pollen tube growth by glucose might optimize the response of pollen tubes to directional cues. If this hypothesis was true, glucose-insensitive pollen tubes should fertilize especially ovules in the bottom part of the silique. Indeed, when wild-type pistils were given limited amounts of *hxk1.3* pollen, the ratio of seeds in the lower part to seeds in the upper part of the pistil was slightly increased compared with minimal

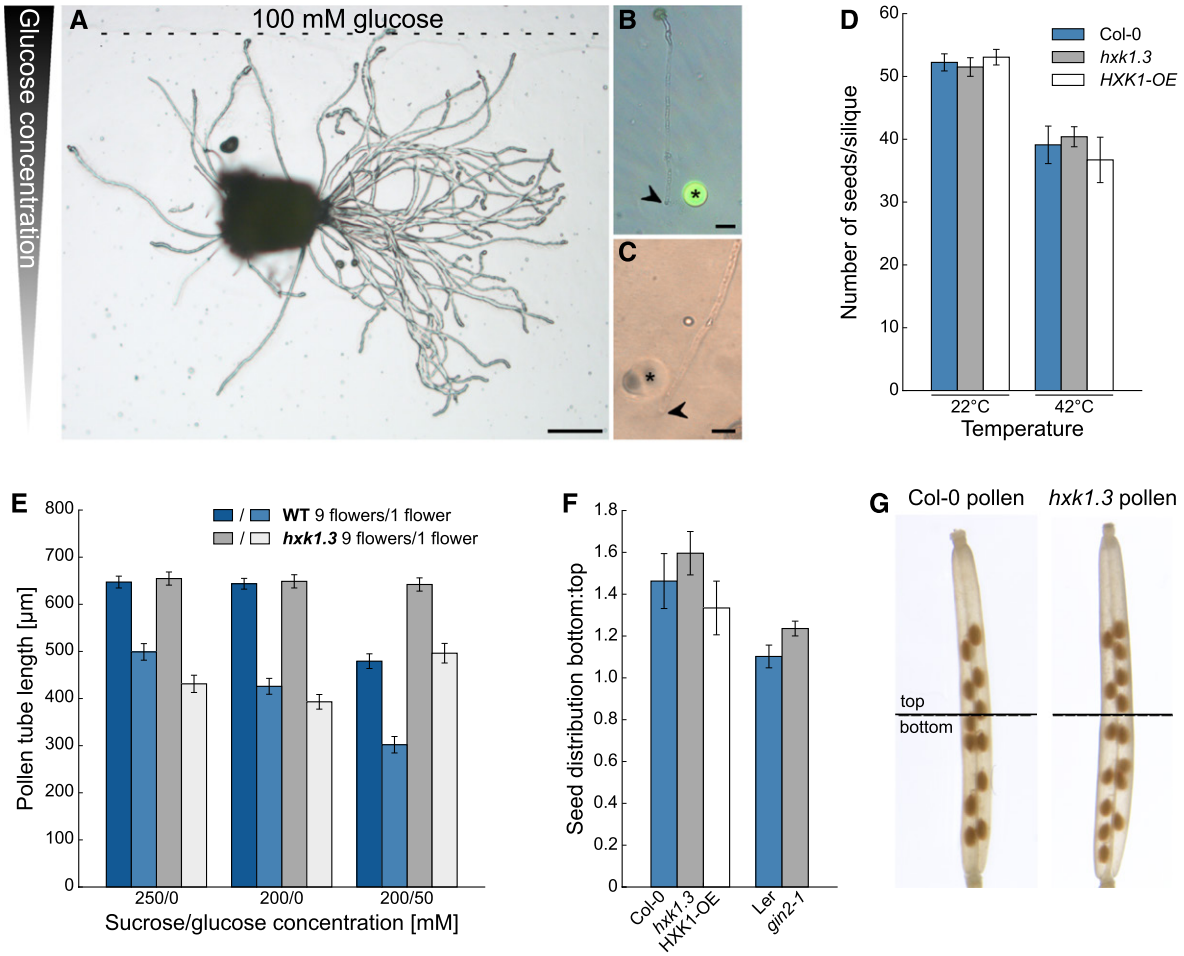


**Figure 10.** Analyses of Hypotheses on the Physiological Functions of Glucose on Pollen Tube Growth.

**(A)** to **(C)** Influence of glucose gradients on pollen tube growth direction.

**(A)** Representative image of semi-in vivo growing pollen tubes challenged with a linear glucose gradient in the germination medium. The glucose gradient across the pollen germination medium was established by pipetting gelatin containing 100 mM glucose in a small band along one side of the pollen germination pad at the beginning of the growth assay.

**(B)** and **(C)** Growth of pollen tubes when gelatin beads containing 500 mM glucose (asterisk) were placed in close proximity to the pollen tube tips (arrowheads). In **(B)**, carboxyfluorescein was added in addition to the gelatin beads to monitor possible diffusion.

**(D)** Number of seeds produced by Col-0, *hxk1.3*, or *HXK1*-OE plants under normal conditions (22°C) and after heat stress (42°C for 3 h). $n \geq 10$ siliques from different plants for every genotype under each temperature condition.

**(E)** Mean lengths ± SE of *hxk1.3* and wild-type pollen tubes germinated in vitro for 7 h. Samples were either prepared by spreading the total pollen of one flower or of nine flowers on the cellulosic membrane of the germination media with different sugar concentrations ($n \geq 200$ pollen tubes for each genotype on every sugar concentration).

**(F)** Distribution of seeds in the top and bottom half of Col-0 siliques after pollination with minimal amounts of Col-0, *hxk1.3*, *HXK1-OE*, L*er*, or *gin2-1* pollen. Means ± SE of three independent experiments with $n \geq 50$ siliques of every genotype in total. Independent experiments were performed with different pistil and pollen donor plants on different days.

**(G)** Representative image of siliques pollinated with limited amounts of Col-0 or *hxk1.3* pollen. Top and bottom part as defined for the measurements shown in **(F)** are indicated.

pollination with Col-0 pollen (Figures 10F and 10G). The same was true for *gin2-1* pollen and the respective wild-type L*er* (Figure 10F). Consistently, minimal pollination with *HXK1*-overexpressing pollen led to the formation of more seeds in the top half of the silique (Figure 10F). However, as these effects were only marginal, further signals are probably involved in the targeting of pollen tubes toward individual ovule positions and the glucose effect on pollen tube growth might influence other so far untested aspects of pollen tube function.

## DISCUSSION

This article (1) characterizes the specific growth inhibition of Arabidopsis pollen tubes by glucose as a signaling molecule, (2)

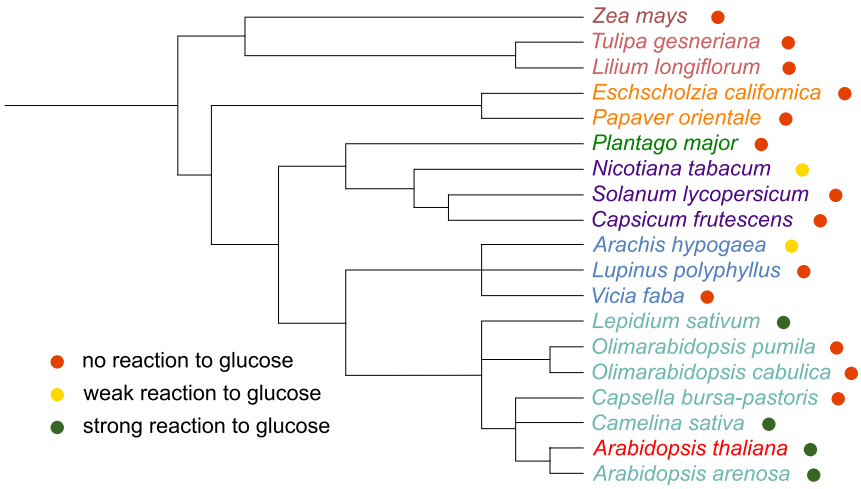


**Figure 11.** Influence of Glucose on Pollen Tube Growth of Different Plant Species.

Pollen of different species were germinated in vitro on media (Supplemental Table 12) with or without glucose and imaged after ~7 h. Length measurements of three biological replicates (different plants and different days) for every species were performed to analyze which species have glucose-sensitive pollen tubes. A slight but not significant reduction of pollen tube growth in the presence of glucose was classified as "weak reaction to glucose." Significant reduction of pollen tube growth was classified as "strong reaction." The results are graphically indicated in a phylogenetic tree depicting all species tested to indicate their relationships. The phylogenetic tree was generated using phyloT (https://phylot.biobyte.de/) and visualized in iTOL (Letunic and Bork, 2016) using already existing phylogenetic information from the NCBI Taxonomy Browser (https://www.ncbi.nlm.nih.gov/Taxonomy/Browser/wwwtax.cgi).

elucidates the involvement of glucose transporters and sugar sensors in this process, and (3) provides a possible model for crosstalk between signaling and pollen tube nutrition.

### Glucose Reduces the Growth Rate of Pollen Tubes via HXK1-Dependent Signaling

Length measurements of pollen tubes grown in vitro on medium supplemented with glucose revealed an inhibitory effect of glucose on pollen tube elongation. Time-curve analyses of pollen tube growth showed that the reduction of final pollen tube length was caused by a decreased growth rate on glucose-containing medium, whereas the observed growth rate of 3.2 μm/min on glucose-free medium was well in line with published growth rates of Arabidopsis pollen tubes in vitro (Wilhelmi and Preuss, 1996; Schiøtt et al., 2004). As pollen tubes grew normally on medium supplemented with L-glucose, mannitol, or fructose in the same concentrations, an osmotic effect of glucose could be excluded as reason for the growth inhibition.

Furthermore, pollen tube growth of *gin2-1* or *hxk1.3* plants was not inhibited in the presence of even high glucose concentrations. As *gin2-1* and *hxk1.3* are defective in glucose signaling (Moore et al., 2003; Aki et al., 2007; Hsu et al., 2014; Rottmann et al., 2016), this points rather toward a signaling function of glucose. It has been known for a long time that sugars not only serve as nutrients but have an additional function as signaling molecules in microorganisms, animals, and plants.

In higher plants, over 2000 genes are regulated by sugars via a complex network of sugar sensing and signaling (Aguilera-Alvarado and Sánchez-Nieto, 2017). There is evidence for signaling pathways induced by sucrose (Wind et al., 2010), trehalose-6-phosphate (Müller et al., 1999), UDP-glucose (Janse van Rensburg and Van den Ende, 2018), glucose (Rolland et al., 2002), and fructose (Cho and Yoo, 2011), which are involved in the regulation of diverse physiological processes (Zhou et al., 1998; Sami et al., 2016). Although sucrose is the main transport sugar in plants, most sugar signaling effects are probably mediated by monosaccharides, especially glucose (Rolland et al., 2006). A central role in glucose signaling is assigned to hexokinases. As moonlighting enzymes, they not only catalyze the first step of glycolysis by phosphorylation of hexoses but also work as glucose sensors in various developmental processes. HXK1 was identified as a glucose sensor by analysis of *gin2-1* plants, which carry a point mutation in *HXK1* and are, in contrast to wild-type plants, able to germinate in the presence of high glucose concentrations (Moore et al., 2003). The observed glucose insensitivity of pollen tubes of *gin2-1* and *hxk1.3* as well as the glucose hypersensitivity of *HXK1*-overexpressing pollen tubes indicated that also in pollen tubes glucose acts as a signal molecule and is perceived by HXK1.

### *HXK1* Is Highly Expressed in Pollen

An important function of HXK1 for the male gametophyte was further underlined by the detection of HXK1 in pollen and growing pollen tubes by reporter gene analysis. Interestingly, qPCR data revealed the highest expression level of *HXK1* in young anthers, while expression in mature pollen and pollen tubes was quite low. Microscopy analyses of anthers of *HXK1*$_{pro}$:*HXK1*g-*GFP* plants showed that *HXK1* expression in anthers

starts in flower buds of stage 9 with the beginning of petal elongation and is confined to developing pollen.

In contrast to the qPCR data, HXK1-GFP and HXK1-GUS showed signals in mature pollen and growing pollen tubes in intensities comparable to signals in young anthers. This indicated that *HXK1* is transcribed and translated mainly during microgametogenesis and that the resulting protein is stable during pollen germination and tube growth. Such a preloading of pollen grains has also been observed for STP8 (Rottmann et al., 2018b) and might be a prearrangement for the immediate use of these proteins at the onset of pollen germination.

This hypothesis was supported by the observation that the growth rate reduction of pollen tubes in response to glucose was induced during the first hours of pollen germination. Pollen tubes germinated semi-in vivo that came in contact with high glucose concentrations only after germination were not inhibited. Previous analysis of *HXK1* expression by semiquantitative RT-PCR had shown a basal level of transcription in all organs (Balasubramanian et al., 2007), which could be confirmed by both reporter gene analysis and qPCR.

However, the expression level of *HXK1* in anthers was >12-fold higher than in roots and seedlings, where the effect of HXK1 in glucose signaling was previously observed (Moore et al., 2003). This points toward a pivotal role of HXK1-mediated glucose sensing in pollen germination and pollen tube function. However, the transduction of the *hxk1.3* mutant allele in cross-pollination experiments with pollen of heterozygous *hxk1.3* plants showed that the inability to sense glucose via HXK1 did not reduce pollen fertility in vivo under standard cultivation conditions.

By contrast, *hxk1.3* pollen tubes showed reduced growth through the stigma and transmitting tract in a pollen tube race experiment. The stress applied to the plant by wounding of the maternal tissue during pistil cutting might have generated conditions that induced the glucose signaling cascade. This indicates that growth inhibition of pollen tubes via glucose signaling might be induced only under certain conditions for example multiple environmental stress, which is the normal situation for Arabidopsis in nature.

The lower number of *hxk1.3* pollen tubes being first to exit a cut style when "racing" against wild-type pollen tubes could theoretically also be interpreted as an increased targeting of ovules by *hxk1.3* pollen under these "stress" conditions. However, this still would indicate that the ability to sense glucose influences the function of the male gametophyte.

### Glucose Sensing in Pollen Tubes Is Independent of the Catalytic Activity of HXK1

Due to its double function, HXK1 can mediate the further transfer of glucose signals in two ways. Some glucose responses depend on the catalytic activity of HXK1, for example, the induction of *PR* genes (Xiao et al., 2000). The second pathway that accounts for the glucose-induced repression of photosynthesis genes or the glucose-induced inhibition of seedling development is independent of the kinase function of HXK1 (Xiao et al., 2000; Moore et al., 2003). This has been shown by restoration of the glucose sensitivity of germinating *gin2-1* plants after transformation with constructs for catalytically inactive $HXK1_{S177A}$ and $HXK1_{G104D}$ point mutants (Moore et al., 2003).

As the transformation of *hxk1.3* with $HXK1_{S177A}$ under the control of the pollen-specific *LAT52* promoter restored glucose sensing in pollen tubes, the underlying glucose signaling is probably also independent of the kinase function of HXK1. Cho et al. (2006) reported that small amounts of HXK1 are in the nucleus, where they form a complex with VHA-B1, RPT5B, and several transcription factors to directly regulate the expression of target genes. In pollen tubes of the $HXK1_{pro}$:*HXK1*g-*GFP* line, GFP signals were detected only at mitochondria, which is the main subcellular localization of HXK1 due to a N-terminal hydrophobic membrane anchor domain of ~24 amino acids (Damari-Weissler et al., 2007). However, this does not exclude the possibility that a small subset of HXK1-GFP may be localized in the nucleus, but at levels below the detection limit by GFP.

In rice (*Oryza sativa*), glucose sensors OsHXK5 and OsHXK6 are also localized at mitochondria, but deletion of the membrane anchor leads to accumulation of the proteins in the nucleus (Cho et al., 2009). It may therefore be the case that glucose leads to the dissociation of a small subset of HXK1 from the mitochondrial membrane, which then enters the nucleus and forms the nuclear HXK1 complex to modulate the expression of glucose response genes. Furthermore, it has been discussed that HXK1 can transfer glucose signals from both subcellular localizations (Balasubramanian et al., 2008).

### Under Optimized in Vitro Conditions Glucose Does Not Inhibit Pollen Germination

Hirsche et al. (2017) reported an HXK1-mediated reduction of pollen germination in vitro on medium containing between 6 and 60 mM glucose. This is in contrast with our results, where only high concentrations of glucose (>75 mM) slightly reduced pollen germination rates. This difference might be explained by the composition of the pollen germination media used. Hirsche et al. (2017) grew pollen on a pollen germination medium containing only $CaCl_2$, $H_3BO_3$, and sucrose, whereas in this study, the medium described by Rodriguez-Enriquez et al. (2013) was used, which contains GABA, myo-inositol, spermidine, $Ca(NO_3)_2$, KCl, casein enzymatic hydrolysate, and ferric ammonium citrate in addition to $CaCl_2$, $H_3BO_3$ and sucrose to optimize pollen germination and tube growth.

The observed differences on the two media are comparable to the medium dependence observed for the glucose inhibition during seed germination. Reduction of MS salts in the medium reduced the threshold concentration for the inhibition of seedling development from 6 to 2% glucose (Cho et al., 2010) and led to changes in the signal transduction pathway. As a reduced pollen germination was also reported on the simple medium in the presence of the phosphorylatable hexoses fructose, mannose, and 2-deoxyglucose, but not on medium with nonphosphorylatable L-glucose, 3-*O*-methylglucose, or 6-deoxyglucose (Hirsche et al., 2017), the reduction of pollen germination rates could be based on the catalytic activity of HXK1.

By contrast, complementation of *hxk1.3* with the catalytically inactive point mutated variant $HXK1_{S177A}$ showed that pollen tube

growth inhibition in the presence of glucose was independent of the kinase activity of HXK1. Differences in the pH of the pollen germination media might also partially explain the contrasting results reported by Hirsche et al. (2017). STPs work as $H^+$-symporters and the extracellular pH has been shown to greatly influence their transport activity (Boorer et al., 1994; Rottmann et al., 2016, 2018b). Therefore, even slight changes in the pH value of the pollen germination medium could result in altered glucose uptake and thus influence the reaction of pollen to glucose.

### Pollen Tubes Contain Glucose in Low Micromolar Concentrations

The glucose concentration of 25 mM required for the inhibition of pollen tube growth is quite low compared with the concentrations of 2 to 6% (111–333 mM) described for the glucose-dependent inhibition of seedling development (Moore et al., 2003; Cho et al., 2010). However, neither of these values reflect the glucose concentrations in the cytosol, where glucose sensing by HXK1 takes place. The $K_d$ value of HXK1 for glucose binding is only 89 μM (Feng et al., 2015).

To measure the changes in cytosolic glucose concentration upon external glucose application, constructs for FRET-based glucose nanosensors (Deuschle et al., 2006) were expressed in pollen tubes. Measurements with different affinity variants of these FLIPglu sensors revealed that pollen tubes take up glucose from the medium in the low micromolar range. This observation is well in line with the $K_d$ value of HXK1. A comparison with FLIPglu measurements in other tissues indicated that glucose levels in pollen tubes are lower than those in mesophyll or root cells (Deuschle et al., 2006), which may point to a high glucose turnover and a low glucose storage capacity of pollen tubes.

After removal of glucose from the medium during FLIP measurements cytosolic glucose levels returned rapidly to the initial concentration. This might be due to further metabolization or compartmentalization of glucose. Glucose might, for example, be translocated into the vacuole by the pollen tube-localized tonoplast monosaccharide transporters AtVGT1, AtTMT1, and AtTMT2 (Wormit et al., 2006; Aluri and Büttner, 2007).

### Glucose Uptake into Pollen Tubes Is Mediated by Numerous STPs

Uptake of sugars into pollen tubes has also been measured in other species like tobacco, *T. paludosa*, or lily (Mascarenhas, 1970; Deshusses et al., 1981; Goetz et al., 2017). In lily, sugar uptake was furthermore reported to be mediated by sugar-proton symport (Deshusses et al., 1981). The observed changes of glucose concentrations in the low micromolar range for Arabidopsis pollen tubes are comparable to the $K_m$ values of monosaccharide proton symporters of the STP family. Indeed, expression of several *STP*s in pollen tubes had previously been detected by different methods (Truernit et al., 1996; Schneidereit et al., 2003, 2005; Scholz-Starke et al., 2003; Rottmann et al., 2016, 2018b) and was confirmed by RT-PCR analysis of pollen tube-derived mRNA preparations for *STP4*, *STP6*, *STP8*, *STP9*, *STP10*, and *STP11* (this work), indicating that these STPs might be responsible for glucose uptake into pollen tubes prior to glucose sensing via HXK1.

An induction of expression during growth through the stigma as reported for some members of the sucrose transporter family (Qin et al., 2009; Leydon et al., 2013) was not observed. This might be explained by the preloading of pollen grains with STP transcripts or proteins. The expression of most *STP*s in pollen tubes is initiated prior to pollen germination. mRNAs of *STP4*, *STP6*, *STP9*, and *STP11* as well as STP8 proteins accumulate in mature pollen, whereas expression in growing pollen tubes is low (Truernit et al., 1996; Schneidereit et al., 2003, 2005; Scholz-Starke et al., 2003; Rottmann et al., 2018b). Only *STP10* expression is first induced during pollen germination and tube growth (Rottmann et al., 2016).

The presence of STP transporters in germinating pollen grains coincides with the expression pattern of *HXK1* and further supports the hypothesis that STPs take up glucose, which is sensed by HXK1 in an early stage of pollen germination. Uptake of glucose into the cytosol of pollen tubes via STPs requires their localization in the plasma membrane. This had already been shown for STP8 and STP10 (Rottmann et al., 2016, 2018b) and was confirmed for STP4, STP6, STP9, and STP11 in this study.

So far, no pollen-specific phenotype for one of the pollen STPs has been described. However, on glucose containing medium all *stp* knockout lines showed a slight increase of pollen tube length compared with wild-type plants. This is astonishing as one would expect that the loss of one out of six glucose transporters in pollen tubes could be complemented by the activity of the remaining five. However, this may be explained by the slightly different temporal expression patterns and transport characteristics of the individual STPs. Accordingly, the stepwise decrease of STPs in double up to sextuple knockout lines led to continuously longer pollen tubes of the respective plants on glucose containing medium.

Such an additive effect of the knockout of *STP*s has also been observed for *stp1* and *stp13*. Both *stp1* and *stp13* plants showed reduced uptake of glucose and fructose into roots but the effect was more prominent in *stp1-13* double knockout plants (Yamada et al., 2011). However, the reduced glucose sensitivity of the multiple knockout lines was not completely additive. This might be caused by the upregulation of the still functional *STP*s, which was shown for different *stp* triple knockout lines by qPCR.

The upregulation of the gene for an STP with possible redundant function has also been described for *stp14* knockout lines, which show an upregulation of *STP4* (Poschet et al., 2010). The low remaining glucose sensitivity and thus glucose uptake activity of *stp4-6-8-9-10-11* pollen tubes might accordingly be caused by the upregulation of *STP*s that are usually not expressed in pollen tubes.

*STP* expression is in general very dynamic and regulated by different signals and processes, for example, by diurnal rhythms (Stadler et al., 2003; Büttner, 2010; Poschet et al., 2010), pathogens (Truernit et al., 1996; Fotopoulos et al., 2003; Nørholm et al., 2006; Lemonnier et al., 2014), abiotic stresses (Yamada et al., 2011), or sugars. A sugar-dependent downregulation has been observed for *STP1*, *STP4*, *STP10*, *STP13*, and *STP14* (Price et al., 2004; Büttner, 2010; Poschet et al., 2010; Cordoba et al., 2015; Rottmann et al., 2016), and in this study, we demonstrated that

also *STP8* is downregulated in pollen tubes in the presence of high glucose concentrations. For *STP4*, *STP8*, and *STP10* that are expressed in pollen tubes, the downregulation is HXK1 dependent (Rottmann et al., 2016) as it no longer occurs in *gin2-1* or *hxk1.3* plants, indicating that there is a feedback regulation of glucose uptake via STPs. After glucose uptake sensing and signaling via HXK1 slows down pollen tube growth and subsequently downregulates *STP* genes.

### Extracellular Fructose:Glucose Ratio Discriminates between Nutritional and Signaling Glucose

In addition to the six genes encoding monosaccharide transporters of the STP family, Arabidopsis pollen tubes express genes for the sucrose transporters AtSUC1, AtSUC3, AtSUC6, AtSUC8, and AtSUC9 (Stadler et al., 1999; Meyer et al., 2004; Leydon et al., 2013; Rottmann et al., 2018a), the polyol/monosaccharide transporters AtPMT1 and AtPMT2 (Klepek et al., 2010), inositol transporters INT1, INT2, and INT4 (Schneider et al., 2007, 2008), and the cell wall invertases cwINV2 and cwINV4 (Hirsche et al., 2009; Ruhlmann et al., 2010). The coexistence of sucrose transporters, cell wall invertases, and monosaccharide transporters was also shown for other species like petunia, tobacco, potato (*Solanum tuberosum*), and lily (Singh and Knox, 1984; Ylstra et al., 1998; Lemoine et al., 1999; Maddison et al., 1999). This indicates that pollen tubes can take up sucrose as well as its cleavage products fructose and glucose, which has been shown by radioactive uptake measurements for tobacco pollen tubes (Goetz et al., 2017).

The extracellular cleavage of sucrose by invertases and the uptake of the resulting monosaccharides could contribute to a quick reduction of the sucrose concentration in the transmitting tract. This would promote the long-distance transport of sucrose from the source leaves to the transmitting tract by increasing the concentration gradient between source and sink and thus ensure a supply of carbohydrates to growing pollen tubes. However, the inhibitory effect of glucose on pollen tube growth seemed to contradict this hypothesis as the cleavage of sucrose by invertases leads to increased glucose concentrations.

Interestingly, the addition of glucose and fructose to the germination medium in equimolar amounts—resembling the fructose to glucose ratio after sucrose cleavage by invertases—allowed normal pollen tube growth rates comparable to those on medium with sucrose as sole carbon source. Consistently, also the glucose-induced downregulation of *STP4*, *STP8*, and *STP10* (Rottmann et al., 2016; this study) was not seen, when pollen tubes were grown on medium with equimolar amounts of both monosaccharides. This indicates that fructose can inhibit the glucose-dependent downregulation of pollen tube growth and provides a possibility for the plant to distinguish between glucose for nutritional purposes derived from sucrose cleavage by cell wall invertases and glucose as signaling molecule.

One possible mechanism to discriminate between the presence of glucose alone or glucose plus fructose would be an interplay between the fructose-sensing pathway and HXK1. In seedlings, fructose sensing is mediated by the fructose sensor FINS1/FBP as seeds of *fins1* mutants are, in contrast to wild-type seeds, able to germinate and develop in the presence of high fructose concentrations (Cho and Yoo, 2011). By contrast, the crosstalk between glucose and fructose signaling in pollen tubes did not involve FINS1 as fructose still complemented the inhibitory effect of glucose in pollen tubes of *fins1* mutants. However, in contrast to findings reported for seedling development, the addition of fructose did not interfere with pollen tube growth, which further suggests that the underlying signaling pathways may be different. The possibility that fructose might block the uptake of glucose via STPs was ruled out by analyses of $^{14}$C-glucose uptake in the presence of high fructose concentrations into yeast cells expressing different *STP*s. This is in line with previous studies showing no considerable fructose transport via STP4, STP8, STP9, STP10, and STP11 (Truernit et al., 1996; Schneidereit et al., 2003, 2005; Rottmann et al., 2016, 2018b).

Of the pollen tube-localized STPs, only STP6 might account for fructose uptake into the cells (Scholz-Starke et al., 2003). Even when considering a possible contribution of AtPMT1 and AtPMT2 to fructose import into pollen tubes (Klepek et al., 2010), probably less fructose than glucose is taken up. The intracellular fructose to glucose ratio for complementation of the glucose inhibition effect may therefore differ from the exogenous 1:1 ratio. However, the molecular mechanism underlying the fructose:glucose ratio sensing remains elusive. A direct impact of fructose on HXK1 seems unlikely, although this enzyme is involved in the metabolism of both glucose and fructose. However, HXK1 has an ~100-fold higher affinity for glucose compared with fructose (Gonzali et al., 2002; Cho and Yoo, 2011).

### SWEET1, 9, and 10 May Mediate Carbohydrate Export into the Apoplast of the Ovary

As flowers are sink organs with only little endogenous photosynthetic activity, it is generally accepted that most carbohydrates supplied to pollen and pollen tubes from the sporophytic tissue are delivered from source tissues via the phloem. Using phloem-mobile fluorescent tracers, Werner et al. (2011) showed that transported metabolites are unloaded from the phloem and delivered into gynoecium wall cells and the stigma including the papillae by symplastic diffusion. To make carbohydrates available to pollen and growing pollen tubes they have to be exported into the apoplastic space. Analysis of *SWEET9*$_{pro}$*:SWEET9*g-*GUS* plants showed that this plasma membrane localized sucrose export carrier is in addition to the already reported localization in nectaries (Lin et al., 2014) also present in the stigma where it might be involved in the release of sucrose toward germinating pollen tubes. GUS reporter plants of *SWEET10* revealed the expression of this gene for a sucrose exporter in anthers and pistils. In anthers, SWEET10 might be involved in the release of sucrose as carbon supply for uptake into developing pollen grains. Comparably, it has already been shown that SWEET8 releases glucose from the tapetum as a carbohydrate supply for pollen (Guan et al., 2008). In the pistil, SWEET10 was localized mainly in the vicinity of the vasculature of the style, where it could release sucrose delivered via the phloem into the apoplast toward growing pollen tubes. Even though carbohydrate analysis in the apoplastic fluid of the Arabidopsis transmitting tract has not been possible so far, data from other species indicate

that the extracellular matrix surrounding the pollen tubes is rich in nutrients (Konar and Linskens, 1966; Loewus and Labarca, 1973). However, the extracellular sucrose provided by SWEET9 and SWEET10 activity is probably mainly a nutrient for the pollen tubes and not a signal. Moreover, its cleavage by invertases would not lead to glucose signaling as glucose and fructose are produced in equimolar amounts. Glucose signaling would require an excess of glucose in the extracellular space of the transmitting tract. This could be provided by direct release of the monosaccharide from cells of the transmitting tissue. Microarray data predicted the expression of the gene for the glucose-specific sugar efflux carrier SWEET1 in flowers. Analysis of *SWEET1*$_{pro}$*:SWEET1*g-*GUS* plants revealed that SWEET1 is mainly localized in cells of the stigma and style, where it may contribute to the release of excess glucose into the apoplast of the pistil to serve as a signal for pollen tube growth inhibition. The localization of SWEET1 in the upper part of the pistil is consistent with the priming effect of the glucose-induced inhibition of pollen tube growth, which requires the presence of glucose in the early stages of pollen tube growth.

### Sugar Requirements for Pollen Tube Growth Are Highly Species Specific

An inhibitory effect of glucose on seed germination and seedling development has long been known and used for genetic screens (Jang et al., 1997). However, the necessity of high concentrations of sugar in the rhizosphere in these experiments has raised concerns about the physiological relevance (Cho et al., 2010). By contrast, the apoplast of the transmitting tissue is likely to contain high concentrations of sugars and the reduced growth rate of glucose-insensitive pollen tubes in pollen tube race experiments through the pistil clearly points toward a physiological relevance of the glucose-induced inhibition of pollen tube growth. However, comparison of wild-type and *hxk1* knockout pollen tube growth under several conditions that lead to reduced pollen tube growth in vivo (for example, heat stress or low pollination density) revealed that glucose signaling is not involved in these processes. For some species, for example, pearl millet (*Pennisetum glaucum*), it has been suggested that glucose gradients might be directional

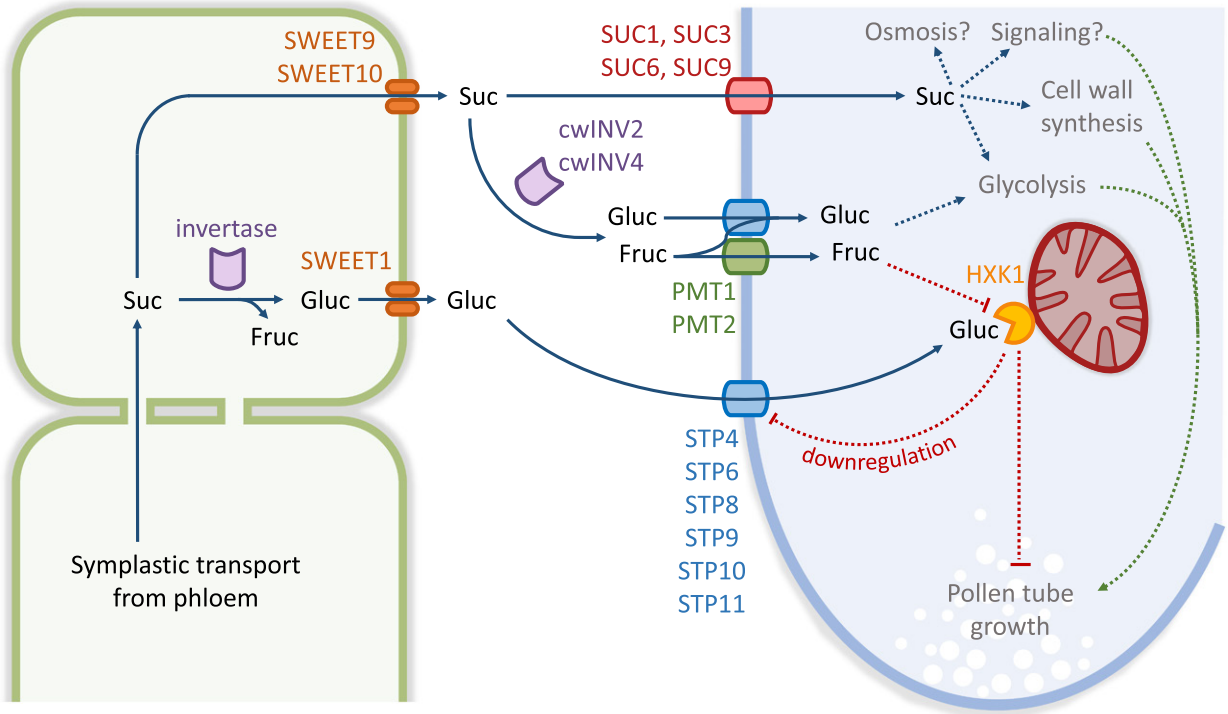


**Figure 12.** Schematic Model of Sugar Supply to Pollen Tubes.

Sucrose delivered into cells of the stigma or transmitting tissue of the style from source tissues is unloaded into the apoplast via SWEET9/SWEET10 or cleaved by intracellular invertases. Sucrose can either be taken up into pollen tubes via SUC transporters or its monosaccharide components are taken up after cleavage by cell wall invertases (cwINV) through PMTs and STPs. Sucrose and monosaccharides derived from extracellular invertase activity contribute to pollen tube growth as signaling molecules, osmotic components or substrates for glycolysis and cell wall synthesis. Release of additional glucose from pistil cells via SWEET1 increases the glucose to fructose ratio in the apoplastic space. After uptake into pollen tubes via STPs glucose activates a signaling pathway through HXK1 localized at mitochondria or in the nucleus. Eventually, this results in the deceleration of pollen tube growth. Activated HXK1 additionally downregulates expression of *STP4*, *STP8*, and *STP10*. In the equimolar presence of glucose and fructose, the glucose signaling pathway is repressed.

cues for pollen tube growth (Reger et al., 1992). In tobacco, a glycoprotein of the transmitting tract displays a glycosylation gradient and stimulates pollen tube growth (Wu et al., 1995). Growth experiments with Arabidopsis pollen tubes on glucose gradients in vitro showed that in this species glucose does not induce changes of pollen tube growth direction. The analysis of pollen tube growth of several plant species from different families on medium supplemented with glucose furthermore revealed that glucose has an inhibitory effect on only few species closely related to Arabidopsis. Furthermore, it has been reported that petunia pollen tubes grow equally well on sucrose- or glucose-containing media (Ylstra et al., 1998) and that increased uptake of glucose even promotes pollen tube growth of cucumber (*Cucumis sativus*; Cheng et al., 2015). Together with the great differences in sugar composition of the in vitro germination media for different species, this indicates that the sugar requirements for pollen germination and tube growth in vivo and probably also the sugar composition of the extracellular matrix of the transmitting tissue are highly species specific. In Arabidopsis, a slight difference between wild-type and glucose-insensitive pollen tubes has been observed in the ovule positions that were fertilized under minimal pollination. This indicates that pollen tube growth might be slowed down by glucose to enable the reaction to directional cues that induce the exit of pollen tubes from the transmitting tract toward the funiculus. A deceleration of pollen tube growth has been observed before pollen tubes enter the micropyle (Stewman et al., 2010), which also requires their reaction to diverse directional signals. As the effects of *hxk1* knockout on targeting of pollen tubes toward ovules was only marginal, further signals are probably involved in this process. On the other hand, the glucose effect on pollen tube growth might influence other so far untested aspects of pollen tube function.

### Model of Sugar Function for Pollen Tube Growth in Arabidopsis

Taken together, the experiments presented here and the current knowledge of carbohydrate transport allow the proposal of a model for sugar supply to pollen tubes and a potential function of sugars as nutrient or signaling molecules (Figure 12). Sucrose is the main transport sugar in Arabidopsis. It is synthesized in source tissues, mainly the mature leaves, and is delivered to the ovary via the phloem. Phloem unloading in ovaries occurs mainly via symplastic diffusion through plasmodesmata (Werner et al., 2011) and provides the cells of the stigma and the transmitting tissue with sucrose. Sucrose can either be directly exported into the apoplast for example via SWEET9/SWEET10 or cleaved by intracellular invertases. Resulting glucose could then be transferred into the apoplast by SWEET1. Apoplastic sucrose can be taken up directly by pollen tubes via sucrose transporters of the SUC family or serve as substrate for the cell wall invertases cwINV2 and cwINV4 of pollen tubes, which leads to the production of glucose and fructose in equimolar amounts. Fructose may be imported into the pollen tube via PMT1, PMT2, and STP6. Glucose is taken up via STP6 and the other pollen tube-localized STPs (STP4, STP8, STP9, STP10, and STP11). After their uptake, these sugars are available for glycolysis and cell wall synthesis or may serve as osmotic compounds or signals for a high energy status, which all promote pollen tube elongation. Additional glucose released into the apoplast during the early phases of pollen tube growth, for example, under multiple stress conditions, is also imported via STPs and detected by the glucose sensor HXK1. As long as glucose and fructose are present in equimolar amounts in the extracellular space, the signaling function of glucose is repressed by fructose in a so far unknown way. Subsequent signaling of HXK1 occurs independently of its catalytic activity and leads to a reduction of the growth velocity of the pollen tube. In a feedback loop, HXK1 eventually mediates the down-regulation of *STP* expression in the presence of high glucose concentrations. Further studies will be necessary to elucidate the processes that lead to the reduction of pollen tube growth after glucose sensing by HXK1.

## METHODS

### Strains, Growth Conditions, and Genotyping

*Arabidopsis thaliana* ecotypes Col-0 and L*er*-0 were grown at 22°C and 60% relative humidity under long-day conditions (16 h of light [white light emitted by metal halide lamps; MT400DL/BH E40] with an intensity of 80 μmol $m^{-2}$ $s^{-1}$/8 h of dark) or in the greenhouse in potting soil. A short-day regime (8 h of light/16 h of dark) was applied to plants used for the generation of protoplasts. For heat shock treatment, flowering plants were incubated for 3 h at 42°C. For the microscopy analysis of roots, plants were grown on MS plates (Murashige and Skoog, 1962). *Arabidopsis arenosa*, *Arachis hypogaea*, *Camelina sativa*, *Capsella bursa-pastoris*, *Capsicum frutescens*, *Eschscholzia californica*, *Lepidium sativum*, *Nicotiana tabacum*, *Olimarabidopsis cabulica*, *Olimarabidopsis pumila*, *Papaver orientale*, *Plantago major*, *Solanum lycopersicum*, and *Vicia faba* were cultivated in the greenhouse in potting soil. Flowers of *Lilium longiflorum* and *Tulipa gesneriana* were obtained from local florists, and *Lupinus polyphyllus* inflorescences were collected from a forest near Erlangen. The T-DNA insertion lines *stp6.1* (SALK_109379; Alonso et al., 2003), *stp8.1* (Wiscseq_DsLox504H01; Woody et al., 2007), *stp9.1* (SALK_142836; Alonso et al., 2003), *stp10.1* (SALK_207063; Alonso et al., 2003), *stp11.1* (GABI_717B07; Kleinboelting et al., 2012), *stp11.2* (CSHL_ET11701; Martienssen and Springer, 2005), *hxk1.1* (SALK_015782; Alonso et al., 2003), *hxk1.2* (SALK_018182; Alonso et al., 2003), *hxk1.3* (SALK_070739; Alonso et al., 2003; Aki et al., 2007; Hsu et al., 2014), and *fins1* (SALK_064456; Alonso et al., 2003; Cho and Yoo, 2011) were obtained from the Nottingham Stock Centre (https://arabidopsis.info/). The *glucose insensitive2-1* (*gin2-1*) mutant line (Moore et al., 2003) was kindly provided by Jen Sheen (Department of Molecular Biology, Massachusetts General Hospital). Homozygous plants were identified by genotyping with the primers listed in Supplemental Table 1. PCR products obtained with the respective primer pairs for the mutant allele were sequenced for the determination of the positions of the T-DNA insertions. Homozygous *stp* multiple knockout lines were generated by crosspollination of different knockout lines and PCR-based genotyping of the F2 descendants. Segregation analysis of the *hxk1.3* allele was also performed by PCR-based genotyping with the primer pairs listed in Supplemental Table 1. *Agrobacterium tumefaciens* strain GV3101 (Holsters et al., 1980; Clough and Bent, 1999) was used for Arabidopsis transformation via floral dip. *Escherichia coli* strains DH5α (Hanahan, 1983) and DB3.1 (Bernard and Couturier, 1992) were used for plasmid cloning. Uptake experiments of $^{14}$C-glucose were

performed with *Saccharomyces cerevisiae* strains derived from strain CSY4000 (Rottmann et al., 2016).

### CRISPR/Cas9-Mediated Knockout of *STP4*

A 20-bp sequence in the third exon of *STP4* was chosen as the protospacer sequence for gene editing (Figure 6A). This sequence is not conserved in the 13 additional Arabidopsis *STP*s and no off-target sites were found when this sequence followed by any of the four protospacer adjacent motif (PAM) sequences (GGG, AGG, TGG, or CGG) was used as query in a nucleotide BLAST analysis of the Arabidopsis genome. Protospacer oligos (Supplemental Table 2) were designed and annealed according to the protocol by Schiml et al. (2016) and inserted into *Bbs*I-digested pEn-Chimera (Fauser et al., 2014). After sequencing, the chimeric sgRNA containing the *STP4*-protospacer was inserted in pDe-CAS9 (Fauser et al., 2014) by LR reaction, yielding expression vector pFC18. pFC18 was used for the transformation of Col-0 wild type as well as *stp6-9-10-11* quadruple knockout plants. BASTA-resistant plants of the T1 generation were tested for the insertion of the sgRNA-*Cas9*-T-DNA by PCR with primers SS43 and Pea3A(T) (Supplemental Table 2). In the T2 generation, individual seedlings that had lost *Cas9* by segregation were identified by PCR with primers SS43 and Pea3A(T). The region surrounding the CRISPR target site was amplified from genomic DNA preparations of these plants with primers STP4+1f and STP4c+851r (Supplemental Table 2). Targeted gene mutations were detected by sequencing of these PCR products. Plants with an identified *STP4* mutation were allowed to self-fertilize and homozygous plants in the T3 generation were detected by sequencing of *STP4* PCR products. To obtain a *stp* sextuple knockout line, *stp6-9-10-11* plants with an identified mutation of *STP4* were crossed with *stp6-8-9-10-11* quintuple knockouts.

### RNA Isolation, Reverse Transcription, and RT-qPCR

Total RNA was extracted from Arabidopsis using TRIzol Reagent (Invitrogen). For RNA isolation from pollen tubes, pollen was either germinated in vitro or semi-in vivo on a cellulosic membrane for at least 5 h (see below). For RNA preparations from stigmatic tissues, unpollinated stigmata were cut off and treated in the same way as the pollen tube samples. Pollen tubes or stigmata were collected by vortex mixing the membrane in 500 µL of TRIzol for 20 s. The QuantiTect reverse transcription kit (Qiagen) was used for the reverse transcription reaction. PCRs for the detection of *STP4*, *STP6*, *STP8*, *STP9*, *STP10*, and *STP11* transcripts in wild-type or mutant cDNA preparations were performed with the primer pairs listed in Supplemental Tables 3 and 4. A PCR with primers specific for *ACTIN2* was performed to confirm the presence of intact cDNA in each sample. Relative expression of *STP4*, *STP8*, *STP10*, *STP11*, and *HXK1* was analyzed via RT-qPCR using the SYBR Green Kit (Agilent) and the Rotor-Gene Q Cycler (Qiagen). Relative expression levels were normalized to the expression level of *UBI10* in each sample and calculated according to the $2^{-\Delta\Delta CT}$ (Livak) method. Gene-specific primers used for RT-qPCR analyses are listed in Supplemental Table 5.

### Generation of the Gateway Destination Vector pTR37

For convenient generation and selection of stable Arabidopsis lines expressing genes of interest under the control of the pollen-specific promoter $LAT52_{pro}$, a new Gateway-compatible destination vector conferring BASTA resistance was cloned. To create pTR37, $LAT52_{pro}$ was amplified from pHD27 (Kost et al., 1998) with the primers $LAT52_{pro}$-8f and $LAT52_{pro}$+639r+AscI (Supplemental Table 6). The resulting 647-bp fragment and all other PCR fragments of this work were confirmed by sequencing. The fragment was inserted into the binary plant expression vector pMDC123_NosT (Rottmann et al., 2016) via *Hind*III/*Asc*I.

### Cloning of Reporter Gene Constructs

For reporter plants expressing *GUS* or *GFP* fusions of *HXK1* under the control of the native promoter, a 2320-bp fragment from the region upstream of *HXK1* was amplified with primers HXK1-3057f+CACC and HXK1-737r (Supplemental Table 7) and cloned into pENTR/D-TOPO (Invitrogen). The second part of the *HXK1* promoter and the genomic sequence including the introns were amplified with the primer pair HXK1-839f and HXK1g+2525r+A+AscI (Supplemental Table 7). The resulting 3364-bp fragment was inserted downstream of the first part of HXK1 via the internal *Mfe*I site and the attached *Asc*I site. The complete $HXK1_{pro}$:*HXK1*g construct was then inserted into pBASTA-GUS or pBASTA-GFP (Rottmann et al., 2016) by the LR reaction, yielding plasmids pTR187 and pTR188, respectively. Constructs for $SWEET1_{pro}$:*SWEET1*g reporter lines were also cloned in two fragments. The first part was amplified with primers SWEET1g-1810f+CACC and SWEET1g-154r, the second part with SWEET1g-488f and SWEET1g+1249r+A+AscI (Supplemental Table 7). Both fragments were united in pENTR/D-TOPO (Invitrogen) via an internal *Eco*RI site and the attached *Asc*I site. LR reaction with the destination vectors pBASTA-GUS or pBASTA-GFP (Rottmann et al., 2016) yielded plasmids pTR14 or pTR15, respectively. The same cloning strategy was applied to *SWEET9* and *SWEET10*. The primer pairs used for amplification of the two fragments of both genes containing the promoter region and the complete genomic sequence are listed in Supplemental Table 7. An internal *Cla*I site was used to ligate both fragments. Complete $SWEET_{pro}$:*SWEET*g constructs were inserted into pBASTA-GUS or pBASTA-GFP, resulting in the expression vectors pTR61 ($SWEET9_{pro}$:*SWEET9*g-*GUS*), pTR62 ($SWEET9_{pro}$:*SWEET9*g-*GFP*), pTR18 ($SWEET10_{pro}$:*SWEET10*g-*GUS*), and pTR19 ($SWEET10_{pro}$:*SWEET10*g-*GFP*).

For analyses of the subcellular localizations of STP4, STP6, and STP9, fusion constructs of the respective coding sequences with *GFP* under the control of the *35S* promoter were generated. To this end, the coding sequences were amplified with the primers listed in Supplemental Table 8. The PCR fragments of *STP4* and *STP9* were cloned into pENTR/D-TOPO (Invitrogen) and inserted into pMDC43 or pMDC83 (Curtis and Grossniklaus, 2003) by the LR reaction, yielding plasmids pTR312 (STP9c-pMDC83) or pTR269 (STP4c-pMDC43). The coding sequence of *STP6* was cloned into pJET1.2/blunt (Thermo Scientific) and then inserted into the *Nco*I site of pSS87 (Schneider et al., 2012b), yielding plasmid pTR12.

The subcellular localization of STP11 was analyzed in tobacco pollen tubes. To allow ligation of the *STP11* coding sequence with the necessary destination vector, an internal *Pci*I restriction site of *STP11* had to be removed by site-directed mutagenesis with mismatching primers (Supplemental Table 8), which introduced a silent point mutation during PCR amplification of *STP11*. The point-mutated *STP11* coding sequence was then ligated into pDD58 (a derivative of pHD27 [Kost et al., 1998] containing the *GFP* sequence of pCS120 [Dotzauer et al., 2010] downstream of the multiple cloning site) via the *Sac*II and *Pci*I sites attached by PCR.

To obtain stable pollen tube marker lines, the coding sequences of *GFP* (pCS120; Dotzauer et al., 2010) and *TagRFP-T* (Shaner et al., 2008) were amplified with the primer pairs listed in Supplemental Table 9. The resulting fragments were ligated into TOPO/pENTR (Invitrogen) and then inserted into pTR37 (see above) downstream of the *LAT52* promoter, yielding plasmids pTR53 (GFP) and pTR80 (TagRFP-T).

### Generation of *HXK1* Overexpression and Complementation Constructs for *hxk1.3*

To complement the pollen tube phenotype of *hxk1.3* mutants, two different constructs were generated. For the complementation construct carrying the wild-type sequence of *HXK1*, the coding sequence was amplified from flower-derived cDNA with the primers HXK1+1f+CACC and

HXK1g+2528r (Supplemental Table 10) and ligated into pENTR/D-TOPO (Invitrogen). Site-directed mutagenesis with mismatching primers (Supplemental Table 10) was then used to replace the serine at position 177 with alanine. Both the wild-type and the *HXK1*$_{S117A}$ fragment were ligated into pTR37 (see above), yielding plasmids pTR258 or pTR262, respectively. The overexpression construct pTR189 was achieved by inserting the whole *HXK1*$_{pro}$*:HXK1*g sequence (see above) into pMDC123_nosT (Rottmann et al., 2016).

### Constructs for the Pollen Tube-Specific Expression of Glucose Nanosensor Genes

Plasmids pRSET-FLIPglu-3.2mΔ13 (#13560), pRSET-FLIPglu-600μΔ13 (#13559), pRSET-FLIPglu-2μΔ13 (#13561), and pRSET-FLIPglu-170nΔ13 (#13562) (Deuschle et al., 2005, 2006) were obtained from Wolf Frommer (Division Molecular Physiology, HHU Düsseldorf) via Addgene. The coding sequences for the nanosensors were amplified with the primers listed in Supplemental Table 11 and ligated into pENTR/D-TOPO (Invitrogen). "Donor only" and "acceptor only" control plasmids were generated by site-directed mutagenesis of FLIPglu-2μΔ13 with mismatch primers (Supplemental Table 11) exchanging either tyrosine at position 67 of eYFP or tryptophan at position 67 of eCFP to glycine, respectively. All FLIP constructs were then inserted downstream of *LAT52*$_{pro}$ in pTR37 (see above) by LR reactions. The resulting plasmids pTR49 (FLIPglu-170nΔ13), pTR50 (FLIPglu-2μΔ13), pTR51 (FLIPglu-600μΔ13), pTR52 (FLIPglu-3.2mΔ13), pTR231 FLIPglu-2μΔ13-donor-only), and pTR234 (FLIPglu-2μΔ13-acceptor-only) were used for the transformation of Col-0 wild-type plants.

### Isolation and Transformation of Arabidopsis Mesophyll Protoplasts

Protoplasts were generated from Col-0 plants as described by Drechsel et al. (2011). After transformation via the polyethylene glycol method (Abel and Theologis, 1994) protoplasts were incubated for ~40 h at 22°C in the dark prior to microscopy analysis.

### Transformation of Pollen by Particle Bombardment

For the analysis of GFP fusion constructs in pollen tubes, *N. tabacum* cv Petit Havana pollen were transiently transformed by particle bombardment as described (Kost et al., 1998). Pollen grains were collected by vortex mixing anthers in liquid germination medium. The grains were then distributed on pollen germination medium solidified with phytagel directly prior to bombardment. Particle bombardment was performed using a helium-driven particle accelerator (PDS-1000/He; Bio-Rad) with all basic adjustments set according to the manufacturer's recommendations. After bombardment, pollen grains were allowed to germinate during an incubation time of 4 to 6 h at 22°C in the dark prior to confocal analysis.

### Radioactive Uptake Measurements

Yeast strains TRY1031 (STP4), TRY1035 (STP9), TRY1004 (STP10), and TRY1036 (STP11) (Rottmann et al., 2016, 2018b) were used to test the fructose binding capacity of different STPs. Transport tests with $^{14}$C-labeled glucose were performed as described by Sauer and Stadler (1993).

### Analyses of Pollen Germination and Pollen Tube Growth

In vitro pollen germination of Arabidopsis for RNA extraction and growth analysis was done as described (Rodriguez-Enriquez et al., 2013). Unless indicated otherwise 250 mM sucrose was used as the default sugar concentration. Pollen germination rates were counted using ImageJ 1.47 (Schneider et al., 2012a). For length measurements, pollen tubes were usually allowed to grow for at least 7 h, unless indicated otherwise. Pollen tube length was measured with a self-written semiautomatic program in Python (Python Software Foundation) and plotted with Matplotlib (Hunter, 2007), which also was used to produce all other graphs. Pollen tube growth experiments were performed in three biological replicates on three different days and with at least three different plants. Of every individual growth assay 17 to 20 images were acquired and the lengths of at least 10 randomly chosen pollen tubes per image were measured. Statistical analysis was performed in Excel with Student's *t* test (unpaired; two-sided). For the determination of growth rates of individual pollen tubes, pollen grains of Col-0 plants stably expressing *GFP* (pTR53) were germinated in small Petri dishes that were sealed with Parafilm. To test the reaction of pollen tubes to glucose gradients, defined concentrations of glucose were embedded in gelatin beads as described by Okuda et al. (2009). To visualize approximate glucose diffusion, carboxyfluorescein was also added to the gelatin beads. To obtain a linear glucose gradient across the pollen germination medium, gelatin mixed with glucose and carboxyfluorescein was pipetted in a small band along one side of the pollen germination pad.

The medium described by Rodriguez-Enriquez et al. (2013) was also used for semi-in vivo pollen growth assays, which were performed by pollinating stigmata, cutting them off and placing them horizontally onto the cellulosic membrane of the growth medium to allow the outgrowth of the pollen tubes from the cut surface (Palanivelu and Preuss, 2006). To directly compare the growth of wild-type and mutant pollen tubes, one-half of the stigma was pollinated with TagRFP-T-labeled wild-type pollen and the other half with GFP-labeled mutant pollen prior to dissection of the stigma. For experiments requiring minimal pollination, sepals, petals, and anthers were removed from almost open flowers and stigmata were pollinated with a limited amount of pollen grains. After about 2 weeks, siliques were harvested and cleared in 70% ethanol to allow the determination of seed number and position.

Pollen of other species was germinated in vitro for ~7 h. The compositions of the growth media for the various species are listed in Supplemental Table 12.

### Microscopy

GUS plants and pollen tubes for length measurements were analyzed by light microscopy (Zeiss Axioskop; Carl Zeiss Jena). To obtain cross sections of pistils of *SWEET1*$_{pro}$*:SWEET1*g*-GUS* reporter plants the method described for Technovit embedding of roots by Scheres et al. (1994) was applied to GUS stained pistils. Of the embedded tissue 10- to 20-μm sections were prepared on a rotary microtome RM2135 (Leica Microsystems). Protoplasts and *GFP* reporter plants were analyzed on a Leica TCS SPII confocal laser scanning microscope (Leica Microsystems) using a 488-nm argon laser line for excitation. Detection windows ranged from 497 to 526 nm for GFP and from 682 to 730 nm for chlorophyll autofluorescence. Pollen tubes of tobacco transformed by particle bombardment, semi-in vivo grown Arabidopsis pollen tubes expressing *TagRFP-T* or *GFP*, pollen for the analysis of growth rates of individual pollen tubes, and pollen tubes with FLIPglu nanosensors were analyzed on a Leica TCS SP5 confocal laser scanning microscope (Leica Microsystems). GFP was excited at 488 nm and detected between 495 and 548 nm, and RFP was excited at 561 nm and detected between 570 and 620 nm. The detection window for chlorophyll autofluorescence of stigmata ranged from 637 to 750 nm. To determine the growth rate of individual pollen tubes, images were taken every 4 s. Pollen tube tracking and calculation of growth velocities were done using a self-written program in Python (Python Software Foundation). For microscopy analyses of pollen tubes with FLIPglu nanosensors, pollen tubes were grown semi-in vivo. Pollinated stigmata were cut off and placed directly on germination medium (without cellulosic membrane) in the perfusion chamber of a custom-made microscope slide (Supplemental Figure 2). After positioning of the stigmata, the

medium was overlaid with a thin film of liquid pollen germination medium and as soon as the pollen tubes emerged from the cut surface the whole chamber of the slide was filled with liquid germination medium. Semi-in vivo pollen tubes expressing the donor only and acceptor only controls were cultivated in the same chamber. Ratio imaging was performed using the 25× dip-in objective and the Leica FRET Sensitized Emission Wizard application according to the method described in the protocol available at https://www.leica-microsystems.com/fileadmin/academy/2012/Application_Letters/Appl_Let_20_FRET_SE_Sep06.pdf. The donor (eCFP) was excited at 458 nm and detected between 465 and 482 nm. Acceptor (eYFP) fluorescence was excited at 514 nm, and the detection window ranged from 520 to 550 nm. Apparent FRET efficiency (E) was calculated in selected regions of interest of the pollen tubes using the formula $E = (B - A * \beta - C * \gamma)/C$ with A, B, and C corresponding to the intensities of the three signals (donor, FRET, and acceptor, respectively) and $\beta$ and $\gamma$ being the calibration factors generated by acceptor only and donor only references (Wouters et al., 2001). Background fluorescence was not subtracted. During time-series recording in 10-s intervals, pollen tubes were constantly perfused with liquid pollen germination medium. Image processing was done using Leica LAS AF software (Leica Microsystems) and GIMP2.8 (https://gimp.org).

### Accession Numbers

Sequence data from this article can be found in the GenBank/EMBL data libraries under accession numbers At3g19930 (STP4), At3g05960 (STP6), At5g26250 (STP8), At1g50310 (STP9), At3g19940 (STP10), At5g23270 (STP11), At4g29130 (HXK1), and At1g43670 (FINS1/FBP).

### Supplemental Data

**Supplemental Figure 1.** Influence of pistil tissues on pollen tube growth.

**Supplemental Figure 2.** Technical setup for the glucose uptake measurements with FLIP nanosensors.

**Supplemental Figure 3.** Characterization of *stp6*, *stp9*, and *stp11* T-DNA insertion lines.

**Supplemental Table 1.** Primers used for PCR-based genotyping of T-DNA insertion lines.

**Supplemental Table 2.** Oligos used for the generation and analysis of *stp4* knockout lines by CRISPR/Cas9.

**Supplemental Table 3.** List of primers used for the detection of *STP* transcripts in floral tissues by RT-PCR.

**Supplemental Table 4.** Primers used for the detection of *STP* transcripts in T-DNA insertion lines by RT-PCR.

**Supplemental Table 5.** List of primers used for RT-qPCR analysis of *STP4*, *STP8*, *STP10*, *STP11*, and *HXK1* transcript levels.

**Supplemental Table 6.** Primers used for the generation of pTR37, a novel Gateway-compatible destination vector for pollen tube-specific expression of target genes.

**Supplemental Table 7.** List of primers used for generation of *HXK1*$_{pro}$*:HXK1*g-, *SWEET1*$_{pro}$*:SWEET1*g-, *SWEET9*$_{pro}$*:SWEET9*g-, and *SWEET10*$_{pro}$*:SWEET10-GUS* and *-GFP* reporter lines.

**Supplemental Table 8.** List of primers used for generation of *GFP* fusion constructs for the transient expression in protoplasts or *Nicotiana tabacum* pollen tubes.

**Supplemental Table 9.** List of primers used for the generation of stable TagRFP-T and GFP pollen tube marker lines.

**Supplemental Table 10.** List of primers used for the generation of complementation constructs for *hxk1.3*.

**Supplemental Table 11.** List of primers used for pollen tube specific expression constructs of FLIPglu nanosensors and the corresponding donor only and acceptor only controls.

**Supplemental Table 12.** Composition of pollen germination media for different plant species.


## ACKNOWLEDGMENTS

We thank Richard Gerum for help with Python programming and Werner Schneider for the construction of the pollen tube flow chamber. We also thank Jen Sheen for providing the Arabidopsis mutant line *gin2-1*, Franz Klebl and Sabine Schneider for helpful discussions, and Angelika Wolf for perfect plant cultivation.


## AUTHOR CONTRIBUTIONS

R.S. conceived the research plans and supervised the experiments. T.R. performed most of the experiments. C.F. generated the *STP4* CRISPR/*Cas9* constructs and performed the plant transformation. T.R. and R.S. designed the experiments and analyzed the data. T.R. wrote the article with contributions from R.S. N.S. discussed the data and supervised and complemented the writing.

Received May 16, 2018; revised July 10, 2018; accepted August 13, 2018; published August 17, 2018.

## REFERENCES


**Abel, S., and Theologis, A.** (1994). Transient transformation of *Arabidopsis* leaf protoplasts: a versatile experimental system to study gene expression. Plant J. **5:** 421–427.

**Aguilera-Alvarado, G.P., and Sánchez-Nieto, S.** (2017). Plant hexokinases are multifaceted proteins. Plant Cell Physiol. **58:** 1151–1160.

**Aki, T., Konishi, M., Kikuchi, T., Fujimori, T., Yoneyama, T., and Yanagisawa, S.** (2007). Distinct modulations of the hexokinase1-mediated glucose response and hexokinase1-independent processes by HYS1/CPR5 in *Arabidopsis.* J. Exp. Bot. **58:** 3239–3248.

**Alonso, J.M., et al.** (2003). Genome-wide insertional mutagenesis of *Arabidopsis thaliana.* Science **301:** 653–657.

**Aluri, S., and Büttner, M.** (2007). Identification and functional expression of the *Arabidopsis thaliana* vacuolar glucose transporter 1 and its role in seed germination and flowering. Proc. Natl. Acad. Sci. USA **104:** 2537–2542.

**Balasubramanian, R., Karve, A., Kandasamy, M., Meagher, R.B., and Moore, Bd.** (2007). A role for F-actin in hexokinase-mediated glucose signaling. Plant Physiol. **145:** 1423–1434.

**Balasubramanian, R., Karve, A., and Moore, B.D.** (2008). Actin-based cellular framework for glucose signaling by Arabidopsis hexokinase1. Plant Signal. Behav. **3:** 322–324.

**Bedinger, P.** (1992). The remarkable biology of pollen. Plant Cell **4:** 879–887.

**Bernard, P., and Couturier, M.** (1992). Cell killing by the F plasmid CcdB protein involves poisoning of DNA-topoisomerase II complexes. J. Mol. Biol. **226:** 735–745.

**Boorer, K.J., Loo, D.D.F., and Wright, E.M.** (1994). Steady-state and presteady-state kinetics of the H+/hexose cotransporter (STP1) from *Arabidopsis thaliana* expressed in *Xenopus* oocytes. J. Biol. Chem. **269:** 20417–20424.

**Büttner, M.** (2010). The Arabidopsis sugar transporter (AtSTP) family: an update. Plant Biol. (Stuttg.) **12** (suppl. 1): 35–41.

**Chaudhuri, B., Hörmann, F., and Frommer, W.B.** (2011). Dynamic imaging of glucose flux impedance using FRET sensors in wild-type *Arabidopsis* plants. J. Exp. Bot. **62:** 2411–2417.

**Chen, L.Q., et al.** (2010). Sugar transporters for intercellular exchange and nutrition of pathogens. Nature **468:** 527–532.

**Chen, L.-Q., Qu, X.-Q., Hou, B.-H., Sosso, D., Osorio, S., Fernie, A.R., and Frommer, W.B.** (2012). Sucrose efflux mediated by SWEET proteins as a key step for phloem transport. Science **335:** 207–211.

**Cheng, J., Wang, Z., Yao, F., Gao, L., Ma, S., Sui, X., and Zhang, Z.** (2015). Down-regulating CsHT1, a cucumber pollen-specific hexose transporter, inhibits pollen germination, tube growth, and seed development. Plant Physiol. **168:** 635–647.

**Cho, J.-I., et al.** (2009). Role of the rice hexokinases *OsHXK5* and *OsHXK6* as glucose sensors. Plant Physiol. **149:** 745–759.

**Cho, Y.-H., and Yoo, S.-D.** (2011). Signaling role of fructose mediated by FINS1/FBP in *Arabidopsis thaliana.* PLoS Genet. **7:** e1001263.

**Cho, Y.H., Yoo, S.D., and Sheen, J.** (2006). Regulatory functions of nuclear hexokinase1 complex in glucose signaling. Cell **127:** 579–589.

**Cho, Y.-H., Sheen, J., and Yoo, S.-D.** (2010). Low glucose uncouples hexokinase1-dependent sugar signaling from stress and defense hormone abscisic acid and $C_2H_4$ responses in Arabidopsis. Plant Physiol. **152:** 1180–1182.

**Clough, S.J., and Bent, A.F.** (1999). Floral dip: a simplified method for Agrobacterium-mediated transformation of *Arabidopsis thaliana*. Plant J. **16:** 735–743.

**Cordoba, E., Aceves-Zamudio, D.L., Hernández-Bernal, A.F., Ramos-Vega, M., and León, P.** (2015). Sugar regulation of *SUGAR TRANSPORTER PROTEIN 1* (*STP1*) expression in *Arabidopsis thaliana.* J. Exp. Bot. **66:** 147–159.

**Curtis, M.D., and Grossniklaus, U.** (2003). A gateway cloning vector set for high-throughput functional analysis of genes in planta. Plant Physiol. **133:** 462–469.

**Damari-Weissler, H., Ginzburg, A., Gidoni, D., Mett, A., Krassovskaya, I., Weber, A.P.M., Belausov, E., and Granot, D.** (2007). Spinach SoHXK1 is a mitochondria-associated hexokinase. Planta **226:** 1053–1058.

**Derksen, J., Rutten, T., Van Amstel, T., De Win, A., Doris, F., and Steer, M.** (1995). Regulation of pollen tube growth. Acta Bot. Neerl. **44:** 93–119.

**Deshusses, J., Gumber, S.C., and Loewus, F.A.** (1981). Sugar uptake in lily pollen. Plant Physiol. **67:** 793–796.

**Deuschle, K., Okumoto, S., Fehr, M., Looger, L.L., Kozhukh, L., and Frommer, W.B.** (2005). Construction and optimization of a family of genetically encoded metabolite sensors by semirational protein engineering. Protein Sci. **14:** 2304–2314.

**Deuschle, K., Chaudhuri, B., Okumoto, S., Lager, I., Lalonde, S., and Frommer, W.B.** (2006). Rapid metabolism of glucose detected with FRET glucose nanosensors in epidermal cells and intact roots of Arabidopsis RNA-silencing mutants. Plant Cell **18:** 2314–2325.

**Dotzauer, D., Wolfenstetter, S., Eibert, D., Schneider, S., Dietrich, P., and Sauer, N.** (2010). Novel PSI domains in plant and animal H+-inositol symporters. Traffic **11:** 767–781.

**Drechsel, G., Bergler, J., Wippel, K., Sauer, N., Vogelmann, K., and Hoth, S.** (2011). *C*-terminal armadillo repeats are essential and sufficient for association of the plant U-box armadillo E3 ubiquitin ligase SAUL1 with the plasma membrane. J. Exp. Bot. **62:** 775–785.

**Ebrahimi, N., and Sadeghi, R.** (2016). Osmotic properties of carbohydrate aqueous solutions. Fluid Phase Equilib. **417:** 171–180.

**Fauser, F., Schiml, S., and Puchta, H.** (2014). Both CRISPR/Cas-based nucleases and nickases can be used efficiently for genome engineering in *Arabidopsis thaliana.* Plant J. **79:** 348–359.

**Fehr, M., Lalonde, S., Lager, I., Wolff, M.W., and Frommer, W.B.** (2003). *In vivo* imaging of the dynamics of glucose uptake in the cytosol of COS-7 cells by fluorescent nanosensors. J. Biol. Chem. **278:** 19127–19133.

**Feng, J., Zhao, S., Chen, X., Wang, W., Dong, W., Chen, J., Shen, J.-R., Liu, L., and Kuang, T.** (2015). Biochemical and structural study of Arabidopsis hexokinase 1. Acta Crystallogr. D Biol. Crystallogr. **71:** 367–375.

**Fotopoulos, V., Gilbert, M.J., Pittman, J.K., Marvier, A.C., Buchanan, A.J., Sauer, N., Hall, J.L., and Williams, L.E.** (2003). The monosaccharide transporter gene, AtSTP4, and the cell-wall invertase, Atbetafruct1, are induced in Arabidopsis during infection with the fungal biotroph *Erysiphe cichoracearum*. Plant Physiol. **132:** 821–829.

**Goetz, M., Guivarćh, A., Hirsche, J., Bauerfeind, M.A., González, M.-C., Hyun, T.K., Eom, S.H., Chriqui, D., Engelke, T., Großkinsky, D.K., and Roitsch, T.** (2017). Metabolic control of tobacco pollination by sugars and invertases. Plant Physiol. **173:** 984–997.

**Gonzali, S., Alpi, A., Blando, F., and De Bellis, L.** (2002). *Arabidopsis* (HXK1 and HXK2) and yeast (HXK2) hexokinases overexpressed in transgenic lines are characterized by different catalytic properties. Plant Sci. **163:** 943–954.

**Guan, Y.-F., Huang, X.-Y., Zhu, J., Gao, J.-F., Zhang, H.-X., and Yang, Z.-N.** (2008). *RUPTURED POLLEN GRAIN1*, a member of the MtN3/saliva gene family, is crucial for exine pattern formation and cell integrity of microspores in Arabidopsis. Plant Physiol. **147:** 852–863.

**Hanahan, D.** (1983). Studies on transformation of *Escherichia coli* with plasmids. J. Mol. Biol. **166:** 557–580.

**Hirsche, J., Engelke, T., Völler, D., Götz, M., and Roitsch, T.** (2009). Interspecies compatibility of the anther specific cell wall invertase promoters from *Arabidopsis* and tobacco for generating male sterile plants. Theor. Appl. Genet. **118:** 235–245.

**Hirsche, J., García Fernández, J.M., Stabentheiner, E., Großkinsky, D.K., and Roitsch, T.** (2017). Differential effects of carbohydrates on Arabidopsis pollen germination. Plant Cell Physiol. **58:** 691–701.

**Holm, S.O.** (1994). Pollination density - effects on pollen germination and pollen tube growth in *Betula pubescens* Ehrh. in northern Sweden. New Phytol. **126:** 541–547.

**Holsters, M., Silva, B., Van Vliet, F., Genetello, C., De Block, M., Dhaese, P., Depicker, A., Inzé, D., Engler, G., Villarroel, R., Van Montagu, M., and Schell, J.** (1980). The functional organization of the nopaline *A. tumefaciens plasmid* pTiC58. Plasmid **3:** 212–230.

**Hsu, Y.-F., Chen, Y.-C., Hsiao, Y.-C., Wang, B.-J., Lin, S.-Y., Cheng, W.-H., Jauh, G.-Y., Harada, J.J., and Wang, C.-S.** (2014). AtRH57, a DEAD-box RNA helicase, is involved in feedback inhibition of glucose-mediated abscisic acid accumulation during seedling development and additively affects pre-ribosomal RNA processing with high glucose. Plant J. **77:** 119–135.

**Hunter, J.D.** (2007). Matplotlib: A 2D graphics environment. Comput. Sci. Eng. **9:** 90–95.

**Jang, J.C., León, P., Zhou, L., and Sheen, J.** (1997). Hexokinase as a sugar sensor in higher plants. Plant Cell **9:** 5–19.

**Janse van Rensburg, H.C., and Van den Ende, W.** (2018). UDP-glucose: a potential signaling molecule in plants? Front. Plant Sci. **8:** 2230.

**Kakani, V.G., Prasad, P.V.V., Craufurd, P.Q., and Wheeler, T.R.** (2002). Response of *in vitro* pollen germination and pollen tube growth of groundnut (*Arachis hypogaea* L.) genotypes to temperature. Plant Cell Environ. **25:** 1651–1661.

**Kleinboelting, N., Huep, G., Kloetgen, A., Viehoever, P., and Weisshaar, B.** (2012). GABI-Kat SimpleSearch: new features of the *Arabidopsis thaliana* T-DNA mutant database. Nucleic Acids Res. **40:** D1211–D1215.

**Klepek, Y.-S., Volke, M., Konrad, K.R., Wippel, K., Hoth, S., Hedrich, R., and Sauer, N.** (2010). *Arabidopsis thaliana* POLYOL/MONOSACCHARIDE TRANSPORTERS 1 and 2: fructose and xylitol/H+ symporters in pollen and young xylem cells. J. Exp. Bot. **61:** 537–550.

**Konar, R.N., and Linskens, H.F.** (1966). Physiology and biochemistry of the stigmatic fluid of *Petunia hybrida.* Planta **71:** 372–387.

**Kost, B., Spielhofer, P., and Chua, N.-H.** (1998). A GFP-mouse talin fusion protein labels plant actin filaments *in vivo* and visualizes the actin cytoskeleton in growing pollen tubes. Plant J. **16:** 393–401.

**Lemoine, R., Bürkle, L., Barker, L., Sakr, S., Kühn, C., Regnacq, M., Gaillard, C., Delrot, S., and Frommer, W.B.** (1999). Identification of a pollen-specific sucrose transporter-like protein NtSUT3 from tobacco. FEBS Lett. **454:** 325–330.

**Lemonnier, P., Gaillard, C., Veillet, F., Verbeke, J., Lemoine, R., Coutos-Thévenot, P., and La Camera, S.** (2014). Expression of *Arabidopsis* sugar transport protein STP13 differentially affects glucose transport activity and basal resistance to *Botrytis cinerea.* Plant Mol. Biol. **85:** 473–484.

**Letunic, I., and Bork, P.** (2016). Interactive tree of life (iTOL) v3: an online tool for the display and annotation of phylogenetic and other trees. Nucleic Acids Res. **44:** W242–W245.

**Leydon, A.R., Beale, K.M., Woroniecka, K., Castner, E., Chen, J., Horgan, C., Palanivelu, R., and Johnson, M.A.** (2013). Three MYB transcription factors control pollen tube differentiation required for sperm release. Curr. Biol. **23:** 1209–1214.

**Leydon, A.R., Chaibang, A., and Johnson, M.A.** (2014). Interactions between pollen tube and pistil control pollen tube identity and sperm release in the Arabidopsis female gametophyte. Biochem. Soc. Trans. **42:** 340–345.

**Lin, I.W., et al.** (2014). Nectar secretion requires sucrose phosphate synthases and the sugar transporter SWEET9. Nature **508:** 546–549.

**Loewus, F., and Labarca, C.** (1973). Pistil secretion product and pollen tube wall formation. In Biogenesis of Plant Cell Wall Polysaccharides, F. Loewus, ed (New York and London: Elsevier), pp. 175–193.

**Maddison, A.L., Hedley, P.E., Meyer, R.C., Aziz, N., Davidson, D., and Machray, G.C.** (1999). Expression of tandem invertase genes associated with sexual and vegetative growth cycles in potato. Plant Mol. Biol. **41:** 741–751.

**Martienssen, R.A., and Springer, P.S.** (2005). Enhancer and gene trap transposon mutagenesis in Arabidopsis. http://genetrap.cshl.org/traps.html.

**Mascarenhas, J.P.** (1970). A new intermediate in plant cell wall synthesis. Biochem. Biophys. Res. Commun. **41:** 142–149.

**Meyer, S., Lauterbach, C., Niedermeier, M., Barth, I., Sjolund, R.D., and Sauer, N.** (2004). Wounding enhances expression of AtSUC3, a sucrose transporter from Arabidopsis sieve elements and sink tissues. Plant Physiol. **134:** 684–693.

**Moore, B., Zhou, L., Rolland, F., Hall, Q., Cheng, W.-H., Liu, Y.-X., Hwang, I., Jones, T., and Sheen, J.** (2003). Role of the Arabidopsis glucose sensor HXK1 in nutrient, light, and hormonal signaling. Science **300:** 332–336.

**Müller, J., Wiemken, A., and Aeschbacher, R.** (1999). Trehalose metabolism in sugar sensing and plant development. Plant Sci. **147:** 37–47.

**Murashige, T., and Skoog, F.** (1962). A revised medium for rapid growth and bioassays with tobacco tissue cultures. Physiol. Plant. **15:** 473–497.

**Nørholm, M.H.H., Nour-Eldin, H.H., Brodersen, P., Mundy, J., and Halkier, B.A.** (2006). Expression of the Arabidopsis high-affinity hexose transporter STP13 correlates with programmed cell death. FEBS Lett. **580:** 2381–2387.

**Okuda, S., et al.** (2009). Defensin-like polypeptide LUREs are pollen tube attractants secreted from synergid cells. Nature **458:** 357–361.

**Palanivelu, R., and Preuss, D.** (2006). Distinct short-range ovule signals attract or repel *Arabidopsis thaliana* pollen tubes in vitro. BMC Plant Biol. **6:** 7.

**Poschet, G., Hannich, B., and Büttner, M.** (2010). Identification and characterization of AtSTP14, a novel galactose transporter from Arabidopsis. Plant Cell Physiol. **51:** 1571–1580.

**Price, J., Laxmi, A., St Martin, S.K., and Jang, J.-C.** (2004). Global transcription profiling reveals multiple sugar signal transduction mechanisms in Arabidopsis. Plant Cell **16:** 2128–2150.

**Qin, Y., Leydon, A.R., Manziello, A., Pandey, R., Mount, D., Denic, S., Vasic, B., Johnson, M.A., and Palanivelu, R.** (2009). Penetration of the stigma and style elicits a novel transcriptome in pollen tubes, pointing to genes critical for growth in a pistil. PLoS Genet. **5:** e1000621.

**Read, S.M., Clarke, A.E., and Bacic, A.** (1993). Stimulation of growth of cultured *Nicotiana tabacum* W 38 pollen tubes by poly(ethylene glycol) and $Cu_{(II)}$ salts. Protoplasma **177:** 1–14.

**Regan, S.M., and Moffatt, B.A.** (1990). Cytochemical analysis of pollen development in wild-type Arabidopsis and a male-sterile mutant. Plant Cell **2:** 877–889.

**Reger, B.J., Pressey, R., and Chaubal, R.** (1992). *In vitro* chemotropism of pearl millet pollen tubes to stigma tissue: a response to glucose produced in the medium by tissue-bound invertase. Sex. Plant Reprod. **5:** 201–205.

**Rodriguez-Enriquez, M.J., Mehdi, S., Dickinson, H.G., and Grant-Downton, R.T.** (2013). A novel method for efficient in vitro germination and tube growth of *Arabidopsis thaliana* pollen. New Phytol. **197:** 668–679.

**Rolland, F., Moore, B., and Sheen, J.** (2002). Sugar sensing and signaling in plants. Plant Cell **14** (suppl.):S185–S205.

**Rolland, F., Baena-Gonzalez, E., and Sheen, J.** (2006). Sugar sensing and signaling in plants: conserved and novel mechanisms. Annu. Rev. Plant Biol. **57:** 675–709.

**Rottmann, T., Zierer, W., Subert, C., Sauer, N., and Stadler, R.** (2016). *STP10* encodes a high-affinity monosaccharide transporter and is induced under low-glucose conditions in pollen tubes of Arabidopsis. J. Exp. Bot. **67:** 2387–2399.

**Rottmann, T.M., Fritz, C., Lauter, A., Schneider, S., Fischer, C., Danzberger, N., Dietrich, P., Sauer, N., and Stadler, R.** (2018a). Protoplast-esculin assay as a new method to assay plant sucrose transporters: characterization of AtSUC6 and AtSUC7 sucrose uptake activity in Arabidopsis Col-0 ecotype. Front. Plant Sci. **9:** 430.

**Rottmann, T., Klebl, F., Schneider, S., Kischka, D., Rüscher, D., Sauer, N., and Stadler, R.** (2018b). Sugar transporter STP7 specificity for L-arabinose and D-xylose contrasts with the typical hexose transporters STP8 and STP12. Plant Physiol. **176:** 2330–2350.

**Ruhlmann, J.M., Kram, B.W., and Carter, C.J.** (2010). *CELL WALL INVERTASE 4* is required for nectar production in *Arabidopsis.* J. Exp. Bot. **61:** 395–404.

**Sami, F., Yusuf, M., Faizan, M., Faraz, A., and Hayat, S.** (2016). Role of sugars under abiotic stress. Plant Physiol. Biochem. **109:** 54–61.

**Sauer, N., and Stadler, R.** (1993). A sink-specific H+/monosaccharide co-transporter from *Nicotiana tabacum*: cloning and heterologous expression in baker's yeast. Plant J. **4:** 601–610.

**Scheres, B., Wolkenfelt, H., Willemsen, V., Terlouw, M., Lawson, E., Dean, C., and Weisbeek, P.** (1994). Embryonic origin of the *Arabidopsis* primary root and root meristem initials. Development **120:** 2475–2487.

**Schiml, S., Fauser, F., and Puchta, H.** (2016). CRISPR/Cas-mediated site-specific mutagenesis in *Arabidopsis thaliana* using Cas9 nucleases and paired nickases. Methods Mol. Biol. **1469:** 111–122.

**Schiøtt, M., Romanowsky, S.M., Baekgaard, L., Jakobsen, M.K., Palmgren, M.G., and Harper, J.F.** (2004). A plant plasma membrane Ca2+ pump is required for normal pollen tube growth and fertilization. Proc. Natl. Acad. Sci. USA **101:** 9502–9507.

**Schlüpmann, H., Bacic, A., and Read, S.M.** (1994). Uridine diphosphate glucose metabolism and callose synthesis in cultured pollen tubes of *Nicotiana alata* Link et Otto. Plant Physiol. **105:** 659–670.

**Schneider, C.A., Rasband, W.S., and Eliceiri, K.W.** (2012a). NIH Image to ImageJ: 25 years of image analysis. Nat. Methods **9:** 671–675.

**Schneider, S., Schneidereit, A., Udvardi, P., Hammes, U., Gramann, M., Dietrich, P., and Sauer, N.** (2007). Arabidopsis INOSITOL TRANSPORTER2 mediates H+ symport of different inositol epimers and derivatives across the plasma membrane. Plant Physiol. **145:** 1395–1407.

**Schneider, S., Beyhl, D., Hedrich, R., and Sauer, N.** (2008). Functional and physiological characterization of *Arabidopsis INOSITOL TRANSPORTER1*, a novel tonoplast-localized transporter for *myo*-inositol. Plant Cell **20:** 1073–1087.

**Schneider, S., Hulpke, S., Schulz, A., Yaron, I., Höll, J., Imlau, A., Schmitt, B., Batz, S., Wolf, S., Hedrich, R., and Sauer, N.** (2012b). Vacuoles release sucrose via tonoplast-localised SUC4-type transporters. Plant Biol. (Stuttg.) **14:** 325–336.

**Schneidereit, A., Scholz-Starke, J., and Büttner, M.** (2003). Functional characterization and expression analyses of the glucose-specific AtSTP9 monosaccharide transporter in pollen of *Arabidopsis.* Plant Physiol. **133:** 182–190.

**Schneidereit, A., Scholz-Starke, J., Sauer, N., and Büttner, M.** (2005). AtSTP11, a pollen tube-specific monosaccharide transporter in Arabidopsis. Planta **221:** 48–55.

**Scholz-Starke, J., Büttner, M., and Sauer, N.** (2003). AtSTP6, a new pollen-specific H+-monosaccharide symporter from Arabidopsis. Plant Physiol. **131:** 70–77.

**Shaner, N.C., Lin, M.Z., McKeown, M.R., Steinbach, P.A., Hazelwood, K.L., Davidson, M.W., and Tsien, R.Y.** (2008). Improving the photostability of bright monomeric orange and red fluorescent proteins. Nat. Methods **5:** 545–551.

**Sheen, J., Zhou, L., and Jang, J.-C.** (1999). Sugars as signaling molecules. Curr. Opin. Plant Biol. **2:** 410–418.

**Singh, M.B., and Knox, R.B.** (1984). Invertases of *Lilium* pollen: characterization and activity during *in vitro* germination. Plant Physiol. **74:** 510–515.

**Smyth, D.R., Bowman, J.L., and Meyerowitz, E.M.** (1990). Early flower development in Arabidopsis. Plant Cell **2:** 755–767.

**Speranza, A., Calzoni, G.L., and Pacini, E.** (1997). Occurrence of mono- or disaccharides and polysaccharide reserves in mature pollen grains. Sex. Plant Reprod. **10:** 110–115.

**Stadler, R., Truernit, E., Gahrtz, M., and Sauer, N.** (1999). The AtSUC1 sucrose carrier may represent the osmotic driving force for anther dehiscence and pollen tube growth in *Arabidopsis.* Plant J. **19:** 269–278.

**Stadler, R., Büttner, M., Ache, P., Hedrich, R., Ivashikina, N., Melzer, M., Shearson, S.M., Smith, S.M., and Sauer, N.** (2003). Diurnal and light-regulated expression of AtSTP1 in guard cells of *Arabidopsis.* Plant Physiol. **133:** 528–537.

**Stewman, S.F., Jones-Rhoades, M., Bhimalapuram, P., Tchernookov, M., Preuss, D., and Dinner, A.R.** (2010). Mechanistic insights from a quantitative analysis of pollen tube guidance. BMC Plant Biol. **10:** 32.

**Swanson, R., Clark, T., and Preuss, D.** (2005). Expression profiling of Arabidopsis stigma tissue identifies stigma-specific genes. Sex. Plant Reprod. **18:** 163–171.

**Ter-Avanesian, D.V.** (1978). The effect of varying the number of pollen grains used in fertilization. Theor. Appl. Genet. **52:** 77–79.

**Truernit, E., Schmid, J., Epple, P., Illig, J., and Sauer, N.** (1996). The sink-specific and stress-regulated Arabidopsis *STP4* gene: enhanced expression of a gene encoding a monosaccharide transporter by wounding, elicitors, and pathogen challenge. Plant Cell **8:** 2169–2182.

**Truernit, E., Stadler, R., Baier, K., and Sauer, N.** (1999). A male gametophyte-specific monosaccharide transporter in *Arabidopsis.* Plant J. **17:** 191–201.

**Villadsen, D., and Smith, S.M.** (2004). Identification of more than 200 glucose-responsive *Arabidopsis* genes none of which responds to 3-O-methylglucose or 6-deoxyglucose. Plant Mol. Biol. **55:** 467–477.

**Wang, Y., Zhang, W.-Z., Song, L.-F., Zou, J.-J., Su, Z., and Wu, W.-H.** (2008). Transcriptome analyses show changes in gene expression to accompany pollen germination and tube growth in Arabidopsis. Plant Physiol. **148:** 1201–1211.

**Weise, A., Barker, L., Kühn, C., Lalonde, S., Buschmann, H., Frommer, W.B., and Ward, J.M.** (2000). A new subfamily of sucrose transporters, SUT4, with low affinity/high capacity localized in enucleate sieve elements of plants. Plant Cell **12:** 1345–1355.

**Werner, D., Gerlitz, N., and Stadler, R.** (2011). A dual switch in phloem unloading during ovule development in *Arabidopsis.* Protoplasma **248:** 225–235.

**Wilhelmi, L.K., and Preuss, D.** (1996). Self-sterility in *Arabidopsis* due to defective pollen tube guidance. Science **274:** 1535–1537.

**Wind, J., Smeekens, S., and Hanson, J.** (2010). Sucrose: metabolite and signaling molecule. Phytochemistry **71:** 1610–1614.

**Woody, S.T., Austin-Phillips, S., Amasino, R.M., and Krysan, P.J.** (2007). The *WiscDsLox* T-DNA collection: an arabidopsis community resource generated by using an improved high-throughput T-DNA sequencing pipeline. J. Plant Res. **120:** 157–165.

**Wormit, A., Trentmann, O., Feifer, I., Lohr, C., Tjaden, J., Meyer, S., Schmidt, U., Martinoia, E., and Neuhaus, H.E.** (2006). Molecular identification and physiological characterization of a novel monosaccharide transporter from Arabidopsis involved in vacuolar sugar transport. Plant Cell **18:** 3476–3490.

**Wouters, F.S., Verveer, P.J., and Bastiaens, P.I.H.** (2001). Imaging biochemistry inside cells. Trends Cell Biol. **11:** 203–211.

**Wu, H.M., Wang, H., and Cheung, A.Y.** (1995). A pollen tube growth stimulatory glycoprotein is deglycosylated by pollen tubes and displays a glycosylation gradient in the flower. Cell **82:** 395–403.

**Xiao, W., Sheen, J., and Jang, J.C.** (2000). The role of hexokinase in plant sugar signal transduction and growth and development. Plant Mol. Biol. **44:** 451–461.

**Yamada, K., Kanai, M., Osakabe, Y., Ohiraki, H., Shinozaki, K., and Yamaguchi-Shinozaki, K.** (2011). Monosaccharide absorption activity of *Arabidopsis* roots depends on expression profiles of transporter genes under high salinity conditions. J. Biol. Chem. **286:** 43577–43586.

**Ylstra, B., Garrido, D., Busscher, J., and van Tunen, A.J.** (1998). Hexose transport in growing petunia pollen tubes and characterization of a pollen-specific, putative monosaccharide transporter. Plant Physiol. **118:** 297–304.

**Zhou, L., Jang, J.C., Jones, T.L., and Sheen, J.** (1998). Glucose and ethylene signal transduction crosstalk revealed by an *Arabidopsis* glucose-insensitive mutant. Proc. Natl. Acad. Sci. USA **95:** 10294–10299.

**Zinn, K.E., Tunc-Ozdemir, M., and Harper, J.F.** (2010). Temperature stress and plant sexual reproduction: uncovering the weakest links. J. Exp. Bot. **61:** 1959–1968.